From Pathophysiology to Treatment of Diabetic Retinopathy 2021

Lead Guest Editor: Irini Chatziralli
Guest Editors: Maria Vittoria Cicinelli and Sara Touhami

From Pathophysiology to Treatment of Diabetic Retinopathy 2021

From Pathophysiology to Treatment of Diabetic Retinopathy 2021

Lead Guest Editor: Irini Chatziralli
Guest Editors: Maria Vittoria Cicinelli and Sara Touhami

Chief Editor

Contents

Research Article

The Impact of Systolic Blood Pressure, Pulse Pressure, and Their Variability on Diabetes Retinopathy among Patients with Type 2 Diabetes

Qingqing Lou [iD],[1] **Xue Chen,**[2] **Kun Wang** [iD],[1] **Huanhuan Liu** [iD],[3] **Zongjun Zhang** [iD],[4] **and Yaujiunn Lee**[5]

[1]*Department of Endocrinology, The First Affiliated Hospital of Hainan Medical University, Haikou, 570102 Hainan, China*
[2]*Jiangsu College of Nursing, Huaian, 223023 Jiangsu, China*
[3]*Department of Endocrinology, Hainan General Hospital, Haikou, 570311 Hainan, China*
[4]*Radiology Department, Affiliated Hospital of Integrated Traditional Chinese and Western Medicine, Nanjing University of Chinese Medicine, Nanjing, 210028, Jiangsu Province, China*
[5]*Lee's Clinic, No. 396, Guangdong RD, Pingtung City, Pingtung County, 900, Taiwan*

Correspondence should be addressed to Qingqing Lou; 2444890144@qq.com and Zongjun Zhang; 13814020968@139.com

Objectives. To evaluate the effects of variations in systolic blood pressure (SBP) and pulse pressure (PP) on diabetic retinopathy (DR) in patients with type 2 diabetes. *Methods*. A total of 3275 type 2 diabetes patients without DR at Taiwan Lee's United Clinic from 2002 to 2014 were enrolled in the study. The average age of the patients was 65.5 (±12.2) years, and the follow-up period ranged from 3 to 10 years. Blood pressure variability was defined as the standard deviation (SD) of the average blood pressure values over the entire study period and was calculated for each patient. The mean SD for SBP was 11.16, and a SBP ≥ 130 mmHg (1 mmHg = 0.133 kPa) was defined as high SBP. Based on these data, patients were divided into four groups as follows: group 1 (G1, mean SBP < 130 mmHg, SD of SBP < 11.16 mmHg), group 2 (G2, mean SBP < 130 mmHg, SD ≥ 11.16 mmHg), group 3 (G3, mean SBP ≥ 130 mmHg, SD of SBP < 11.16 mmHg), and group 4 (G4, mean SBP ≥ 130 mmHg, SD ≥ 11.16 mmHg). Based on a mean PP of 80 mmHg with a pulse pressure SD of 6.53 mmHg, the patients were regrouped into four groups designated G1′-G4′. *Results*. After adjusting for patient age, sex, and disease course, Cox regression showed that the mean and SD of SBP, pulse pressure, and their SDs were risk factors for DR. After stratifying the patients based on the mean and SD of the SBP, we found that the patients in the G4 group had the highest risk of DR (hazard ratio (HR) = 1.980, 95% CI: 1.716~2.285, $P < 0.01$) and patients in the G1 group had the lowest risk. Patients in the G3 group (HR = 1.409, 95% CI: 1.284~1.546, $P < 0.01$) had a higher risk of DR compared to those in the G2 group (HR = 1.353, 95% CI: 1.116~1.640, $P < 0.01$). After the restratification of patients based on the mean and SD of the pulse pressures, it was found that patients in the G2′ group had the highest risk of DR (HR = 2.086, 95% CI: 1.641~2.652, $P < 0.01$), whilst patients in the G1′ group had the lowest risk. Also, the risk of DR in the G4′ group (HR = 1.507, 95% CI: 1.135~2.000, $P < 0.01$) was higher than that in the G3′ group (HR = 1.289, 95% CI: 1.181~1.408, $P < 0.01$). *Conclusions*. Variability in SBP and PP are risk factors for DR in patients with type 2 diabetes. The variability of PP was better able to predict the occurrence of DR than mean pulse pressure.

1. Introduction

Blood pressure variability (BPV), also known as blood pressure fluctuation, refers to the degree of fluctuation in blood pressure within a certain time. Quantification of BPV usu- ally uses the SD of blood pressure readings measured over a certain time to indicate the degree of overall changes in blood pressure during that period. BPV is often indepen- dent of the average blood pressure levels and is closely related to cardiovascular and cerebrovascular damage in

diabetes patients where high variability indicates cardiovascular and cerebrovascular damage [1, 2].

Diabetic retinopathy (DR) is a common microvascular complication and an important cause of vision damage and blindness in diabetes patients [3–5]. Hypertension, mainly high SBP [6, 7] and high PP [8], is a recognized risk factor for DR; however, recent studies have shown that BPV is also associated with DR in diabetes patients [9, 10]. Hata et al. [11] conducted a multicenter study in Europe showing that systolic BPV is an independent risk factor for DR in patients with type 2 diabetes mellitus (T2DM). However, in Asian patients with T2DM, the relationship between SBP, PP variability, and DR remains unclear. In this study, we aimed to evaluate the impact and variability of SBP and PP on DR in patients with T2DM.

2. Materials and Methods

2.1. Subjects. This was a prospective cohort study. Diabetes patients who visited Taiwan Lee's United Clinics from 1 January 2002 to 30 December 2014 were enrolled in the study. Patients were followed up for 3 to 10 years, with patients requested to have four follow-up visits per year. If a patient did not come for the visit as scheduled, the health care professionals would remind the patient to come to the clinics. Patients with a follow-up period less than 3 years ($n = 557$), those with blood pressure measurements taken fewer than three times per year ($n = 402$), those with missing or incomplete data ($n = 1378$), and those who did not have T2DM ($n = 428$) were excluded from the study. Finally, 3275 patients without DR at baseline were included in the study. This study was approved by the Ethics Committee of the Affiliated Hospital of Integrated Traditional Chinese and Western Medicine of Nanjing University and the Taiwan Lee's United Clinic, China (19-053-B). All participants recruited to the study provided written informed consent.

2.2. Data Collection. Data were collected from the database including the following: (1) demographic and clinical data, including age, sex, diabetes course, smoking, drinking, exercise habits, medication (hypoglycemic drugs, insulin, lipid-lowering drug, hypoglycemic drugs, and hypotensive drugs), height, weight, waist circumference, hip circumference, body mass index (BMI), waist-to-hip ratio, systolic pressure, diastolic pressure, and pulse pressure, and (2) laboratory data, including fasting blood that was collected every quarter (after fasting overnight for more than 8 hours). High-performance liquid chromatography (DCCT-aligned) was used to measure glycated hemoglobin A1c (HbA1c). A Roche Cobas600 automatic biochemical analyzer was used to measure the levels of total cholesterol (TC), triglyceride (TG), high-density lipoprotein cholesterol (HDL-C), and low-density lipoprotein cholesterol (LDL-C). (3) Direct ophthalmoscopy after mydriasis was performed by an ophthalmologist. The presence of microaneurysm, cotton wool spots, intracavitary microvascular abnormalities, bleeding, hard exudate, venous aneurysm, or new retinal blood vessels was defined as DR [12]. During the follow-up period, the same procedure was conducted annually.

2.3. Evaluation of Mean Blood Pressure and BPV. Blood pressure values with a systolic pressure in the range of 50-300 mmHg (1 mmHg = 0.133 kPa), diastolic pressure in the range of 30-180 mmHg, and PP in the range of 20-120 mmHg were recognized as effective measurement values [9]. The mean value of multiple blood pressure measurements taken from the same patient on the same day was taken as the measurement value for that day. Mean arterial pressure (MAP) was calculated as (SBP + 2 × diastolic blood pressure)/3SD. The BPVs were defined as SD from the average blood pressure [13] by calculating average values of systolic, diastolic, and pulse pressure and MAP measurements and their SDs for each participant during the entire study period.

2.4. Patient Grouping. A mean SD of SBP of 11.16, and a SBP ≥ 130 mmHg (1 mmHg = 0.133 kPa) were defined as high SBP. Based on these data, all the patients ($n = 3275$) were divided into four groups as follows: G1 (mean SBP < 130 mmHg, SD of SBP < 11.16 mmHg), G2 (mean SBP < 130 mmHg, SD ≥ 11.16 mmHg), G3 (mean SBP ≥ 130 mmHg, SD of SBP < 11.16 mmHg), and G4 (mean SBP ≥ 130 mmHg, SD ≥ 11.16 mmHg). Based on a mean PP of 80 mmHg and a SD of the PP of 6.53 mmHg, the 3275 patients were regrouped into four groups designated G1′-G4′: G1′ (mean PP < 80 mmHg, SD of PP < 6.53 mmHg), G2′ (mean PP < 80 mmHg, SD ≥ 6.53 mmHg), G3′ (mean PP ≥ 80 mmHg, SD of PP < 6.53 mmHg), and G4′ (mean PP ≥ 130 mmHg, SD of PP ≥ 6.53 mmHg).

2.5. Statistical Analysis. SPSS 22.0 software was used for statistical analysis. Count data were expressed as the number of cases (%), and a χ^2 test was used for comparisons between the groups. When the measurement data were normally distributed, the data were expressed as mean ± SD, and an independent sample t-test was used to compare the difference between two groups. Nonnormally distributed data were expressed as medians (upper and lower quartile), and a nonparametric test was used for intergroup comparisons. Cox regression analysis was used to analyze the relationship between different blood pressure variables and the development of DR. As we grouped patients into G1-G4 according to their SPB and SD of SBP and G1′-G4′ according to their PP and SD of PP to compare between the different groups, G1 and G1′ served as the reference in the COX regression models. Covariates including age, sex, course of the disease, BMI, waist-to-hip ratio, HbA1c, TC, TG, LDL-C, and HDL-C were entered into the models simultaneously. Hazard ratios (HR) and their respective 95% confidence intervals (CI) were calculated. P values of <0.05 were considered statistically significant.

3. Results

3.1. Baseline Characteristics. A total of 3275 patients participated in this study. Based on the results of the fundus mydriasis test, patients were divided into a non-DR (NDR) group (2833 cases) and a DR group (442 cases) in which 100 cases had nonproliferative DR and 342 cases had proliferative DR.

Among the patients with proliferative DR, 247 cases were at the early stage of proliferation, 72 cases were at the fibrotic stage, and 23 cases were at the late stage of proliferation. During follow-up, progression of DR was observed, with 15 patients progressing from nonproliferative to proliferative DR and being in the early stage of proliferation. Thirteen cases progressed from the early proliferative stage to the fibrotic stage, and three patients progressed from the fibrotic stage to the late stage of proliferation. There were no significant differences in sex, BMI, waist-to-hip ratio, smoking history, drinking history, use of lipid-lowering drugs, use of antihypertensive drugs, diastolic blood pressure, MAP, TC, TG, and LDL-C between the NDR and the DR groups ($P > 0.05$). Compared to the NDR group, patients in the DR group were older, had had a longer duration of diabetes, and had poorer exercise habits. They also had a higher incidence of macular edema and cataracts, lower use of hypoglycemic drugs and insulin, and higher levels of HbA1c, SBP, and pulse pressure. The NDR patients also had lower levels of HDL-C. The differences between the groups were all statistically significant ($P < 0.05$, Table 1).

3.2. The Relationship between Blood Pressure and the Risk of DR. After adjusting for age, sex, and disease course, Cox regression showed that a higher mean SBP (hazard ratio (HR) = 1.023, 95% confidence interval (CI): 1.019~1.028, $P < 0.01$), SD of SBP (HR = 1.019, 95% CI: 1.012~1.026, $P < 0.01$), mean PP (HR = 1.009, 95% CI: 1.002~1.016, $P < 0.05$), SD (HR = 1.020, 95% CI: 1.006~1.034, $P < 0.01$), HbA1c (HR = 1.289, 95% CI: 1.257~1.321, $P < 0.01$), higher LDL-C (HR = 1.006, 95% CI: 1.002~1.010, $P < 0.01$), and lower HDL-C (HR = 0.981, 95% CI: 0.976~0.986, $P < 0.01$) were associated with more rapid development of DR (Table 2).

3.3. Cox Regression Analysis after Systolic Pressure Stratification. Cox regression analysis showed that after adjusting for age, sex, course of the disease, BMI, waist-to-hip ratio, HbA1c, TC, TG, LDL-C, and HDL-C, patients in the G4 group had the highest risk of DR (HR = 1.980, 95% CI: 1.716~2.285, $P < 0.01$) and patients in the G1 group had the lowest risk. Also, patients in the G3 group (HR = 1.409, 95% CI: 1.284~1.546, $P < 0.01$) had a higher risk of DR compared to those in the G2 group (HR = 1.353, 95% CI: 1.116~1.640, $P < 0.01$, Figure 1).

3.4. Cox Regression Analysis after PP Stratification. Based on a mean PP of 80 mmHg and a SD of the PP of 6.53 mmHg, the patients were regrouped into four groups designated G1$'$-G4$'$: G1$'$ (mean PP < 80 mmHg, SD of PP < 6.53 mmHg), G2$'$ (mean PP < 80 mmHg, SD ≥ 6.53 mmHg), G3$'$ (mean PP ≥ 80 mmHg, SD of PP < 6.53 mmHg), and G4$'$ (mean PP ≥ 130 mmHg, SD of PP ≥ 6.53 mmHg). After adjusting for age, sex, disease course, BMI, waist-to-hip ratio, HbA1c, TC, TG, LDL-C, and HDL-C, Cox regression analysis showed that patients in the G2$'$ group had the highest risk of DR (HR = 2.086, 95% CI: 1.641~2.652, $P < 0.01$) and patients in the G1$'$ group had the lowest risk. Also, patients in the G4$'$ group (HR = 1.507, 95% CI: 1.135~2.000, $P < 0.01$) had a

higher risk of DR compared to those in the G3$'$ group (HR = 1.289, 95% CI: 1.181~1.408, $P < 0.01$, Figure 1).

3.5. The Relationship between Changes in Blood Pressure and DR. Compared to the other three groups, patients in the G4 group had the highest risk of DR. The risk of DR increased between our study groups when the mean systolic pressure exceeded 130 mmHg, the SD of SBP exceeded 8 mmHg, the mean PP exceeded 70 mmHg, and the SD of PP exceeded 4 mmHg (Figure 2).

4. Discussion

4.1. Variability in SBP and PP Are Risk Factors for DR in T2DM Patients. Studies have shown [14, 15] that an increase in BPV is independent of blood pressure and can aggravate damage to the target organs of hypertension. Therefore, reducing BPV and maintaining a stable blood pressure are as important as lowering blood pressure. The role of BPV in microvascular disease in diabetes patients has also attracted major attention. However, previous studies [16, 17] have been mostly cross-sectional surveys that did not clarify the causal relationship between variability in SBP, pulse pressure, and DR. This study found that variability in SBP and PP were risk factors for DR in patients with T2DM. Foo et al. [12] showed that a higher mean SBP, but not SBP variability, was significantly correlated with the occurrence of DR in patients with T2DM. This is not consistent with our study. There are several possible reasons for the discrepancy. In comparison to our study, Foo et al. used a smaller sample size (398 cases, compared to the 3275 cases in our study) and had a relatively short follow-up time (average of 2 years compared to an average of 7 years). Also, the duration of diabetes (average 10 years versus an average of 20 years in our study) was relatively short. In addition, 70% of the study population was from Eastern Asia and China, with the remaining 30% from Southeast Asia, Malaysia, and India. In our study, the entire population was from Eastern Asia and China. Another study [18] showed that SBP variability was an independent risk factor for T2DM nephropathy but had no effect on DR. These findings may be due to the small sample used (664 cases versus 3275 cases), the short duration of diabetes (average 5 years versus average 20 years), and a low overall mean SBP SD (9.72 mmHg versus 11.16 mmHg).

Although it is currently unclear how SBP and PP affect DR in T2DM patients, it can be hypothesized that increased blood pressure may damage retinal capillary endothelial cells [19]. Studies of retinal physiology have shown that blood pressure has a role in the pathological changes of DR and participates in the local renin-angiotensin system [20]. Controlling blood pressure can avoid hyperperfusion to reduce the possibility of blood vessel shear injury caused by hypertension. Therefore, reducing the damage of high perfusion to the endothelial cells, blood vessels, and surrounding tissues may help to prevent DR.

Diastolic blood pressure is an important blood pressure parameter. In this study, no correlation was found between diastolic blood pressure and DR in T2DM patients which

TABLE 1: Comparison of the general information between the diabetic retinopathy and the nondiabetic retinopathy groups.

Indicators	DR group ($n = 442$)	NDR group ($n = 2833$)	P value
Female (number of cases (%))	239 (54.1)	1425 (50.3)	0.607
Age (years, $\bar{x} \pm s$)	67.5 ± 11.3	65.2 ± 12.4	<0.001
BMI (kg/m^2, $\bar{x} \pm s$)	25.9 ± 4.0	26.2 ± 4.2	0.140
Waist-to-hip ratio ($\bar{x} \pm s$)	0.9 ± 0.10	0.9 ± 0.3	0.938
Diabetes course (years, $\bar{x} \pm s$)	23.2 ± 9.5	16.7 ± 7.6	<0.001
Smoking (cases (%))	126 (28.9)	741 (28.6)	0.473
Drinking (cases (%))	97 (22.2)	623 (24.1)	0.224
Exercise (cases (%))	245 (56.2)	1568 (60.6)	0.048
Macular edema (cases (%))	13 (3.0)	12 (0.5)	<0.001
Cataract (cases (%))	231 (53.0)	695 (26.8)	<0.001
Medication			
Hypoglycemic drugs (cases (%))	352 (80.7)	2 166 (83.7)	<0.001
Insulin (cases (%))	104 (23.9)	726 (28.0)	<0.001
Lipid-lowering drugs (cases (%))	294 (67.4)	1772 (68.4)	0.410
Antihypertensive drugs (cases (%))	196 (45.0)	1183 (45.7)	0.544
HbA$_{1c}$ (%)	8.8 ± 2.0	8.1 ± 1.9	<0.001
Systolic pressure (mmHg, $\bar{x} \pm s$)	138.7 ± 15.7	134.5 ± 16.8	<0.001
Diastolic pressure (mmHg, $\bar{x} \pm s$)	78.2 ± 9.2	77.8 ± 9.7	0.462
Pulse pressure (mmHg, $\bar{x} \pm s$)	82.4 ± 11.1	80.3 ± 12.1	0.001
MAP (mmHg, $\bar{x} \pm s$)	101.7 ± 15.3	100.1 ± 16.6	0.062
TC (mg/dl, $\bar{x} \pm s$)	191.5 ± 41.5	188.9 ± 37.3	0.456
TG (mg/dl, median (upper and lower quartile))	126.00 (87.3, 173.0)	124.0 (88.0, 176.3)	0.645
LDL-C (mg/dl, $\bar{x} \pm s$)	109.1 ± 34.2	104.7 ± 30.8	0.074
HDL-C (mg/dl, $\bar{x} \pm s$)	47.6 ± 12.1	48.5 ± 13.5	0.035

Note: DR: diabetic retinopathy; NDR: nondiabetic retinopathy; BMI: body mass index; HbA$_{1c}$: glycosylated hemoglobin; MAP: mean arterial pressure; TC: total cholesterol; TG: triglycerides; LDL-C: low-density lipoprotein cholesterol; HDL-C: high-density lipoprotein cholesterol. [a]t value; [b]Z value.

TABLE 2: Cox regression analysis of risk factors for diabetic retinopathy.

Variables	HR	95% CI	P value
Mean systolic blood pressure	1.023	1.019~1.028	<0.001
SD of systolic blood pressure	1.019	1.012~1.026	<0.001
Mean diastolic blood pressure	0.986	0.968~1.005	0.151
SD of diastolic blood pressure	0.999	0.994~1.004	0.601
Mean pulse pressure	1.009	1.002~1.016	0.018
SD of pulse pressure	1.020	1.006~1.034	<0.001
Mean MAP	0.992	0.976~1.009	0.381
SD of MAP	0.996	0.983~1.008	0.496
HbA$_{1c}$	1.289	1.257~1.321	<0.001
TC	0.999	0.996~1.003	0.701
TG	0.999	0.999~1.000	0.059
HDL-C	0.981	0.976~0.986	<0.001
LDL-C	1.006	1.002~1.010	<0.001

Note: MAP: mean arterial pressure; HbA1c: glycosylated hemoglobin; TC: total cholesterol; TG: triglycerides; HDL-C: high-density lipoprotein cholesterol; LDL-C: low-density lipoprotein cholesterol; HR: risk ratio; CI: confidence interval. Correction for age, gender, and disease course. HRs were for per 1-unit increase of each continuous variable.

is consistent with the results from Kawasaki et al. [21] and Rudnisky et al. [22]. This may be because the diastolic blood pressure is more reflective of peripheral vascular resistance and so the arterial function is small, whilst the SBP mainly reflects the hemodynamics of the central aorta. Concerning the physiological and pathological mechanism of DR, endothelial dysfunction tends to cause vasoconstriction rather than vasodilation, and changes in low-resistance arteries may be more important compared to large arterial dysfunction.

The variability in SBP and PP is more harmful to DR than the average SBP and pulse pressure. In clinical practice, physicians should avoid drastically lowering the blood pressure of patients over a short time. This is particularly important in China where the insurance strategy for inpatients is better than that for outpatients. Many hypertensive patients prefer to be hospitalized. Reducing the blood pressure from a relatively high level to a near-normal level within an average time of seven days of hospitalization will inevitably lead to an increase in BPV. These changes affect the occurrence of chronic microvascular complications such as DR. Our data support the development of individualized blood pressure reduction programs to smoothly lower blood pressure and reduce BPV.
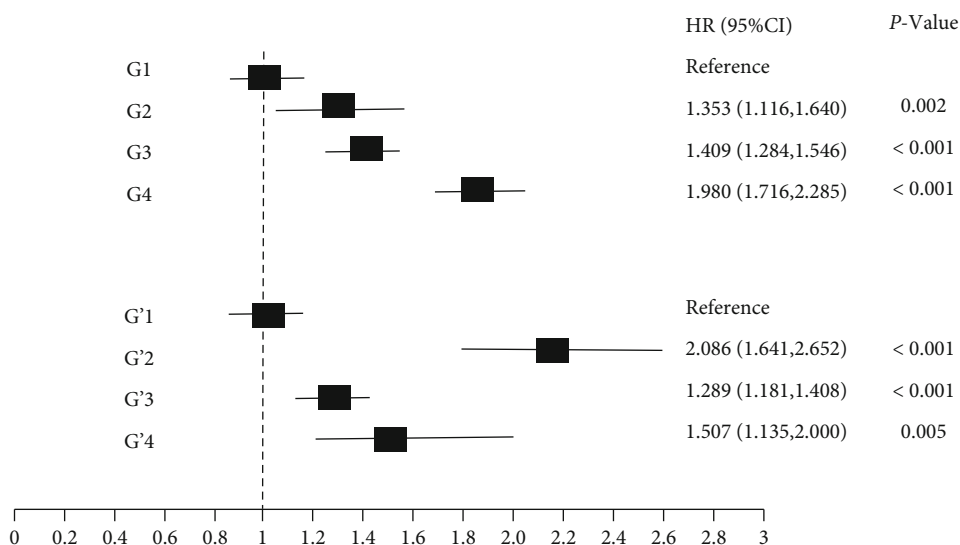
Figure 1: Cox regression on group comparisons. Results were adjusted for age, sex, course of the disease, BMI, waist-to-hip ratio, HbA1c, TC, TG, LDL-C, and HDL-C. G1: mean SBP < 130 mmHg and SD of SBP < 11.16 mmHg; G2: mean SBP < 130 mmHg and SD of SBP ≥ 11.16 mmHg; G3: mean SBP ≥ 130 mmHg and SD of SBP < 11.16 mmHg; G4: mean SBP ≥ 130 mmHg and SD of SBP ≥ 11.16 mmHg. G1$'$: mean PP < 80 mmHg and SD of PP < 6.53 mmHg; G2$'$: mean PP < 80 mmHg and SD of PP ≥ 6.53 mmHg; G3$'$: mean PP ≥ 80 mmHg and SD of PP < 6.53 mmHg; G4$'$: mean PP ≥ 80 mmHg and SD of PP ≥ 6.53 mmHg.
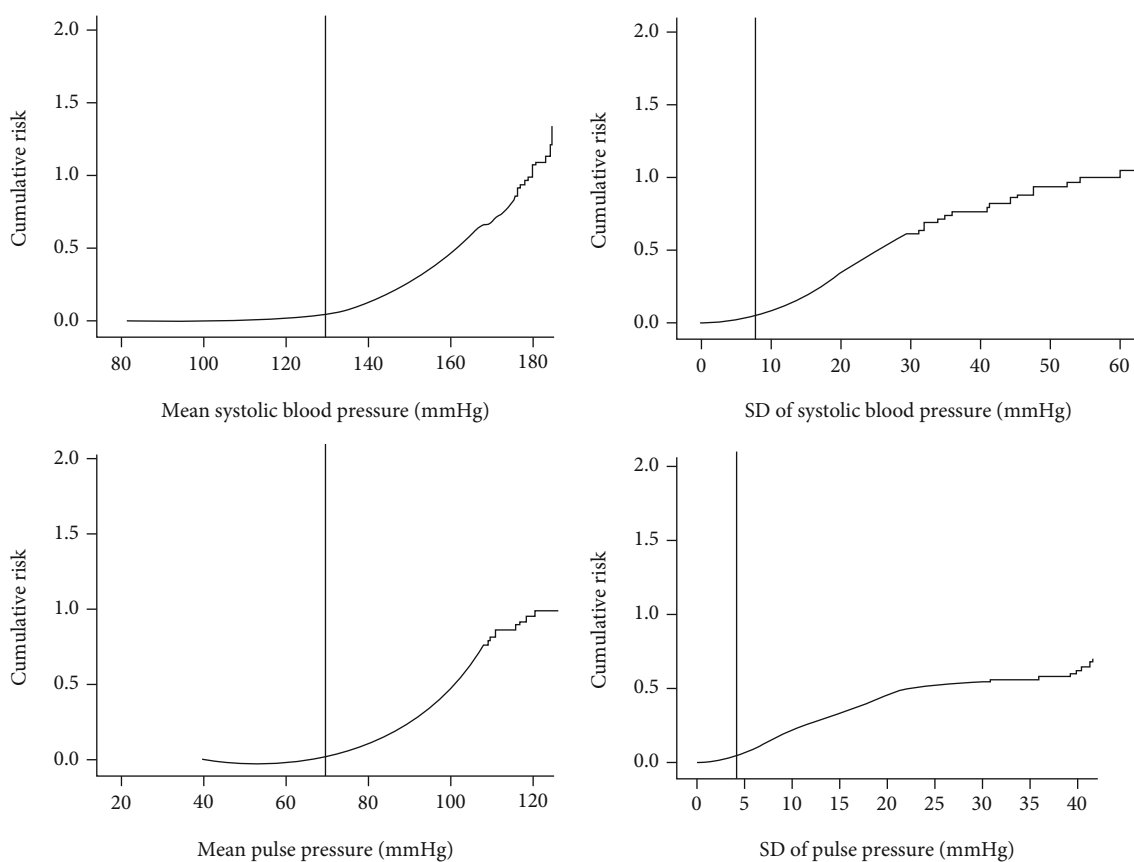
Figure 2: The relationship between systolic blood pressure, pulse pressure, their variability, and diabetes retinopathy.

4.2. The Advantages and Limitations of This Study.

Our study has several advantages in that it was performed as a large prospective longitudinal cohort study with a sufficient sample size. Each patient was followed up for at least three years with an average follow-up time of seven years. Also, at least three independent systolic and PP measurements

were used to calculate the mean systolic and pulse pressures, as well as the variability in the systolic and pulse pressures. These data provided reliable parameters for the mean systolic and PP as well as the variability of systolic and pulse pressure. One of the main limitations of this study was that during the follow-up period, the number and intervals of systolic and PP measurements varied for each subject per year even though they were supposed to be measured every quarter. Also, as our data were only collected from patients with DR, we are not able to determine if the DR was caused by hypertension or by diabetes. No further analysis of the data was performed to focus specifically on hypertensive DR.

In conclusion, variability in SBP and PP are risk factors for DR in patients with T2DM. This variability may be more important than the mean SBP and PP in the development of DR. In the future, individualized blood pressure reduction programs should be considered in clinical practice to slowly lower blood pressure and improve BPV, thereby delaying the risk of chronic complications of diabetes such as DR.

Data Availability

The data used to support the findings of this study are available from the corresponding author upon request.

Disclosure

The funders had no role in the study design, data collection and analysis, decision to publish, or preparation of the paper.

Conflicts of Interest

The authors have no conflicts of interest to declare.

Authors' Contributions

Qingqing Lou and Zongjun Zhang conceived and designed the study. Xue Chen, Kun Wang, and Huanhuan Liu collected the epidemiological and clinical data. Yaujiunn Lee and Huanhuan Liu assisted with patient recruitment and training supervision. Qingqing Lou and Xue Chen drafted the manuscript. Qingqing Lou, Xue Chen, Kun Wang, and Huanhuan Liu contributed to acquisition, analysis, and interpretation of data. Qingqing Lou and Zongjun Zhang contributed to critical revision of the manuscript for important intellectual content. All authors read, revised, and approved the final draft. Qingqing Lou and Zongjun Zhang are the guarantors of this work and, as such, had full access to all the data in the study and take responsibility for the integrity of the data and the accuracy of the data analysis. Qingqing Lou and Xue Chen served as co-first authors.

Acknowledgments

References

[1] G. Parati, J. E. Ochoa, P. Salvi, C. Lombardi, and G. Bilo, "Prognostic value of blood pressure variability and average blood pressure levels in patients with hypertension and diabetes," *Diabetes Care*, vol. 36, no. 2, pp. S312–S324, 2013.

[2] M. Chiriacò, K. Pateras, A. Virdis et al., "Association between blood pressure variability, cardiovascular disease and mortality in type 2 diabetes: a systematic review and meta-analysis," *Diabetes, Obesity & Metabolism*, vol. 21, no. 12, pp. 2587–2598, 2019.

[3] J. W. Yau, S. L. Rogers, R. Kawasaki et al., "Global prevalence and major risk factors of diabetic retinopathy," *Diabetes Care*, vol. 35, no. 3, pp. 556–564, 2012.

[4] S. R. Flaxman, R. R. Bourne, S. Resnikoff et al., "Global causes of blindness and distance vision impairment 1990-2020: a systematic review and meta-analysis," *The Lancet Global Health*, vol. 5, no. 12, pp. e1221–e1234, 2017.

[5] P. Song, J. Yu, K. Y. Chan, E. Theodoratou, and I. Rudan, "Prevalence, risk factors and burden of diabetic retinopathy in China: a systematic review and meta-analysis," *Journal of Global Health*, vol. 8, no. 1, article 010803, 2018.

[6] J. Ding and T. Y. Wong, "Current epidemiology of diabetic retinopathy and diabetic macular edema," *Current Diabetes Reports*, vol. 12, no. 4, pp. 346–354, 2012.

[7] Q. Mohamed, M. C. Gillies, and T. Y. Wong, "Management of diabetic retinopathy," *Journal of the American Medical Association*, vol. 298, no. 8, pp. 902–916, 2007.

[8] M. Yamamoto, K. Fujihara, M. Ishizawa et al., "Pulse pressure is a stronger predictor than Systolic Blood Pressure for severe eye diseases in diabetes mellitus," *Journal of the American Heart Association*, vol. 8, no. 8, article e010627, 2019.

[9] M. Sohn, N. Epstein, E. S. Huang et al., "Visit-to-visit systolic blood pressure variability and microvascular complications among patients with diabetes," *Diabetes Complications*, vol. 31, no. 1, pp. 195–201, 2017.

[10] P. Veloudi, L. Blizzard, V. K. Srikanth et al., "Associations of blood pressure variability and retinal arteriolar diameter in participants with type 2 diabetes," *Diabetes and Vascular Disease Research*, vol. 13, no. 4, pp. 299–302, 2016.

[11] J. Hata, H. Arima, P. M. Rothwell et al., "Effects of visit-to-visit variability in systolic blood pressure on macrovascular and microvascular complications in patients with type 2 diabetes mellitus: the ADVANCE trial," *Circulation*, vol. 128, no. 12, pp. 1325–1334, 2013.

[12] V. Foo, J. Quah, G. Cheung et al., "HbA1c, systolic blood pressure variability and diabetic retinopathy in Asian type 2 diabetics," *Journal of Diabetes*, vol. 9, no. 2, pp. 200–207, 2017.

[13] E. O. M. Gosmanova, M. K. B. Mikkelsen, M. Z. M. P. Molnar et al., "Association of systolic blood pressure variability with mortality, coronary heart disease, stroke, and renal disease," *Journal of the American College of Cardiology*, vol. 68, no. 13, pp. 1375–1386, 2016.

[14] P. M. Rothwell, S. C. Howard, E. Dolan et al., "Prognostic significance of visit-to-visit variability, maximum systolic blood pressure, and episodic hypertension," *Lancet*, vol. 375, no. 9718, pp. 895–905, 2010.

[15] P. E. S. Jennersjö, M. Wijkman, A. Wiréhn et al., "Circadian blood pressure variation in patients with type 2 diabetes-relationship to macro- and microvascular subclinical organ damage," *Primary Care Diabetes*, vol. 5, no. 3, pp. 167–173, 2011.

[16] M. Ishihara, Y. Yukimura, T. Aizawa, T. Yamada, K. Ohto, and K. Yoshizawa, "High blood pressure as risk factor in diabetic retinopathy development in NIDDM patients," *Diabetes Care*, vol. 10, no. 1, pp. 20–25, 1987.

[17] J. Cui, J. P. Ren, D. N. Chen et al., "Prevalence and associated factors of diabetic retinopathy in Beijing, China: a cross-sectional study," *BMJ Open*, vol. 7, no. 8, p. e15473, 2017.

[18] T. Takao, Y. Matsuyama, H. Yanagisawa, M. Kikuchi, and S. Kawazu, "Visit-to-visit variability in systolic blood pressure predicts development and progression of diabetic nephropathy, but not retinopathy, in patients with type 2 diabetes," *Journal of Diabetes and its Complications*, vol. 28, no. 2, pp. 185–190, 2014.

[19] L. Liu, N. D. Quang, R. Banu et al., "Hypertension, blood pressure control and diabetic retinopathy in a large population-based study," *PLoS One*, vol. 15, no. 3, article e229665, 2020.

[20] A. K. Sjølie, P. Dodsonand, and F. R. R. Hobbs, "Does renin-angiotensin system blockade have a role in preventing diabetic retinopathy? A clinical review," *International Journal of Clinical Practice*, vol. 65, no. 2, pp. 148–153, 2011.

[21] R. Kawasaki, S. Tanaka, T. Yamamoto et al., "Incidence and progression of diabetic retinopathy in Japanese adults with type 2 diabetes: 8 year follow-up study of the Japan diabetes complications study," *Diabetologia*, vol. 54, no. 9, pp. 2288–2294, 2011.

[22] C. J. Rudnisky, B. K. Wong, H. Virani, and M. T. S. Tennant, "Risk factors for progression of diabetic retinopathy in Alberta First Nations communities," *Canadian Journal of Ophthalmology*, vol. 47, no. 4, pp. 365–375, 2012.

Research Article

Early Microglial Changes Associated with Diabetic Retinopathy in Rats with Streptozotocin-Induced Diabetes

Young Gun Park,[1] Ji-Yeon Lee,[2] Chongtae Kim,[2] and Young-Hoon Park[1,2]

[1]*Department of Ophthalmology and Visual Science, Seoul St. Mary's Hospital, College of Medicine, The Catholic University of Korea, Seoul, Republic of Korea*
[2]*Catholic Institute for Visual Science, College of Medicine, The Catholic University of Korea, Seoul, Republic of Korea*

Correspondence should be addressed to Young-Hoon Park; parkyh@catholic.ac.kr

Although morphological changes in microglia have been reported to be associated with diabetic retinopathy, little is known about the early changes in the microglia and macrophages during the progression of this condition. The present study was aimed at characterizing retinal microglial activation in the early stages of experimental diabetic retinopathy. Toward this end, a model of diabetic retinopathy was generated by intraperitoneally injecting male Sprague-Dawley rats with streptozotocin. No apparent histological changes were observed during the early stages of experimental diabetic retinopathy. However, at 4 to 16 weeks after the onset of diabetes, the retinas from diabetic rats exhibited higher density of microglia than those from age-matched normal controls, with microglial density peaking at 12 weeks. In particular, the proportion of the activated microglia increased significantly in the diabetic rats, specifically in the nerve fiber and ganglion cell layers, whereas it decreased in the inner plexiform layer within 12 weeks. Furthermore, the resident retinal microglial cells were activated immediately after diabetes induction, peaked at 12 weeks, and remained for up to 16 weeks after disease onset. Thus, experimental diabetic retinopathy causes gradual hypoxia and neuroinflammation, followed by the activation of microglia and the migration of macrophages. The distribution and density of retinal microglial activation changed typically with the progression of the disease in early-stage diabetic rats.

1. Introduction

Diabetic retinopathy (DR) is a major complication of diabetes and a leading cause of blindness, with the severe form of the disease affecting the working-age population on a global scale [1, 2]. Microvascular lesions and inflammation play a crucial role in the pathogenesis of DR. Current accepted pharmacological treatments for DR including diabetic macular edema are intravitreal antivascular endothelial growth factor (VEGF) or steroids [3, 4]. They are administered by intravitreal injection and stabilize the detrimental effects of VEGF on microvascular proliferation and permeability [5].

However, there is a considerable unmet need for proper treatment in the early stages of DR. In recent years, many researchers focused on potential pharmacological targets

for early diagnosis and treatment of DR. Some microRNAs (miRNAs) can regulate gene expression and related signaling pathways. Lazzara et al. reported a dysregulation in the expression of several miRNAs in diabetic mice and displayed their ability to be potent mediators in the pathological mechanisms associated with DR [6, 7]. These can reveal miRNA-gene-pathways that are modulated in the early phase of DR and other microvascular diseases.

Other studies have reported that pathological changes are induced in the retinal neurovascular units prior to vascular injury [8, 9]. Furthermore, microglia are activated and play a pivotal role in DR. Retinal glial activation and neuronal injury have also been reported during the early stages of DR.

Many studies have suggested that microglial activation could be reflected in neuroinflammatory changes. In diabetic

rats, morphological changes in microglia have been reported to occur before neuronal apoptosis and activation of other glial cells in the retina [10, 11]. In a model of streptozotocin- (STZ-) induced diabetes, the expression of retinal Iba-1 was increased by approximately 25%–70%, with a significant difference observed 2 months after diabetes onset [12–14]. Retinal microglial density has been shown to markedly increase in 4-month-old diabetic rats [15].

Although the role of microglia in DR is generally accepted, little is known about the early changes in microglia and macrophages during the progression of DR before chronic damage by ischemia; additionally, chronological changes in the retinal microglia during the early stages of diabetes have not been reported. In the present study, we investigated microglial activation and proliferation during the early course of experimental DR, i.e., before the induction of chronic ischemic damage—to obtain insights into the contribution of these phenomena to DR—using appropriate cell markers.

2. Materials and Methods

2.1. Animals. Male Sprague-Dawley rats (8 weeks old; weighing 250–300 g; Orient Bio Co., Seongnam-si, Gyeonggi-do, Korea) were used in this study. The animals were kept in a plastic cage in a climate-controlled laboratory with a 12 h light/dark cycle. All procedures performed in studies involving animals were in accordance with the ethical standards of the Institutional Animal Care and Use Committee (IACUC) and Department of Laboratory Animals (DOLA) in the Catholic University of Korea where the studies were conducted. The Catholic University of Korea Songeui Campus accredited the Korea Excellence Animal Laboratory Facility from the Korea Food and Drug Administration in 2017 and acquired Association for Assessment and Accreditation of Laboratory Animal Care (AAALAC) International full accreditation in 2018.

All the animal procedures were carried out in accordance with the Laboratory Animals Welfare Act, Guide for the Care and Use of Laboratory Animals, and Guidelines and Policies for Rodent Experiments provided by IACUC in the School of Medicine, the Catholic University of Korea (Approval number: CUMS-2019-0199-06). This article does not contain any studies with human participants performed by any of the authors.

2.2. Induction of Diabetes. A model of diabetes mellitus (DM) was established by a single intraperitoneal injection of STZ (Sigma-Aldrich; 60 mg/kg body weight) in 0.05 M HCl-sodium citrate buffer solution (pH 5.5). The day of STZ injection was defined as day one. The animals were placed in a gas chamber containing 2% isoflurane in oxygen. When unconscious, the animals were removed from the chamber but kept under anesthesia with a mask (1.5% isoflurane in oxygen).

Serum glucose was measured from the tail vein using an automated Accu-Chek glucometer (Roche Diagnostics Ltd., Indianapolis, IN, USA) 3 days following diabetes induction. When serum glucose measured >250 mg/dL on day 3, the development of DM was confirmed, and the rats were used for further experiments. Body weight and serum glucose levels were recorded every week after DM induction.

2.3. Tissue Preparation and Histologic Evaluation. The eyeballs were enucleated under anesthesia with zolazepam and xylazine in an aseptic manner. The posterior halves of the globes were immersed in 4% paraformaldehyde in 0.1 M phosphate buffer, pH 7.4. Whole retinas were dissected and immersed in the same fixative for 2 h. After fixation, the retinas were immersed in 30% sucrose, refrigerated overnight, and then flash-frozen in liquid nitrogen and stored at -70°C for preservation. Five-micrometer-thick sections were stained with hematoxylin and eosin (HE).

2.4. Immunofluorescence Staining. Retinal pieces were trimmed from the central portion of the superior quadrant and rinsed with 0.01 M phosphate-buffered saline (PBS), pH 7.4. After thorough rinsing, the retinal pieces were embedded in 4% agar and cut into 40 μm thick vertical sections. The retinal sections were collected in culture wells and processed using immunofluorescent microscopy. To block nonspecific binding sites, the sections were treated with buffer B (1% BSA, 0.2% bovine gelatin, and 0.05% saponin in 0.01 M PBS) for 3 h on ice. The sections were then incubated with the following antibodies: monoclonal mouse anti-Ki67 (Thermo Fisher Scientific, Waltham, MA, USA; dilution 1 : 1500), monoclonal mouse anti-ED1 (Bio-Rad, Hercules, California, USA; dilution 1 : 100), and polyclonal rabbit anti-Iba1 (Wako, Japan; dilution 1 : 500) overnight at 4°C. After washing with 0.01 M PBS, immunoreactivity was visualized using secondary antibodies including the species-appropriate Cy3-conjugated donkey anti-rabbit IgG (Jackson ImmunoResearch, West Grove, PA, USA; dilution 1 : 3000) and Alexa Fluor 488 donkey anti-mouse conjugated IgG (Life technologies, Grand Island, NY, USA; dilution 1 : 2000) for 2 h at room temperature. Before mounting, cell nuclei were counterstained with 4′,6-diamidine-2′-phenylindole dihydrochloride (DAPI, Thermo Scientific, Waltham, MA, USA; dilution 1 : 1000). After washing in 0.1 M phosphate buffer, the sections were mounted on a glass slide with a mounting medium (Dako, Santa Clara, CA, USA).

2.5. Confocal Microscopy. Immunofluorescent staining was evaluated via confocal laser scanning microscopy (LSM 800 Meta, Carl Zeiss Co. Ltd., Germany). Fluorescent images were captured with red (red: excitation 650 nm, emission 647–700 nm) at 240x, and PEDF images were observed at 400x magnification power. Captured images were converted to JPEG format.

2.6. Statistical Analysis. Statistical analysis for comparison of age-matched control and diabetic groups was performed using ANOVA. In individual age groups, Student's *t*-test with Bonferroni adjustment was used to evaluate the significance of the changes between the age-matched controls and diabetic rats.
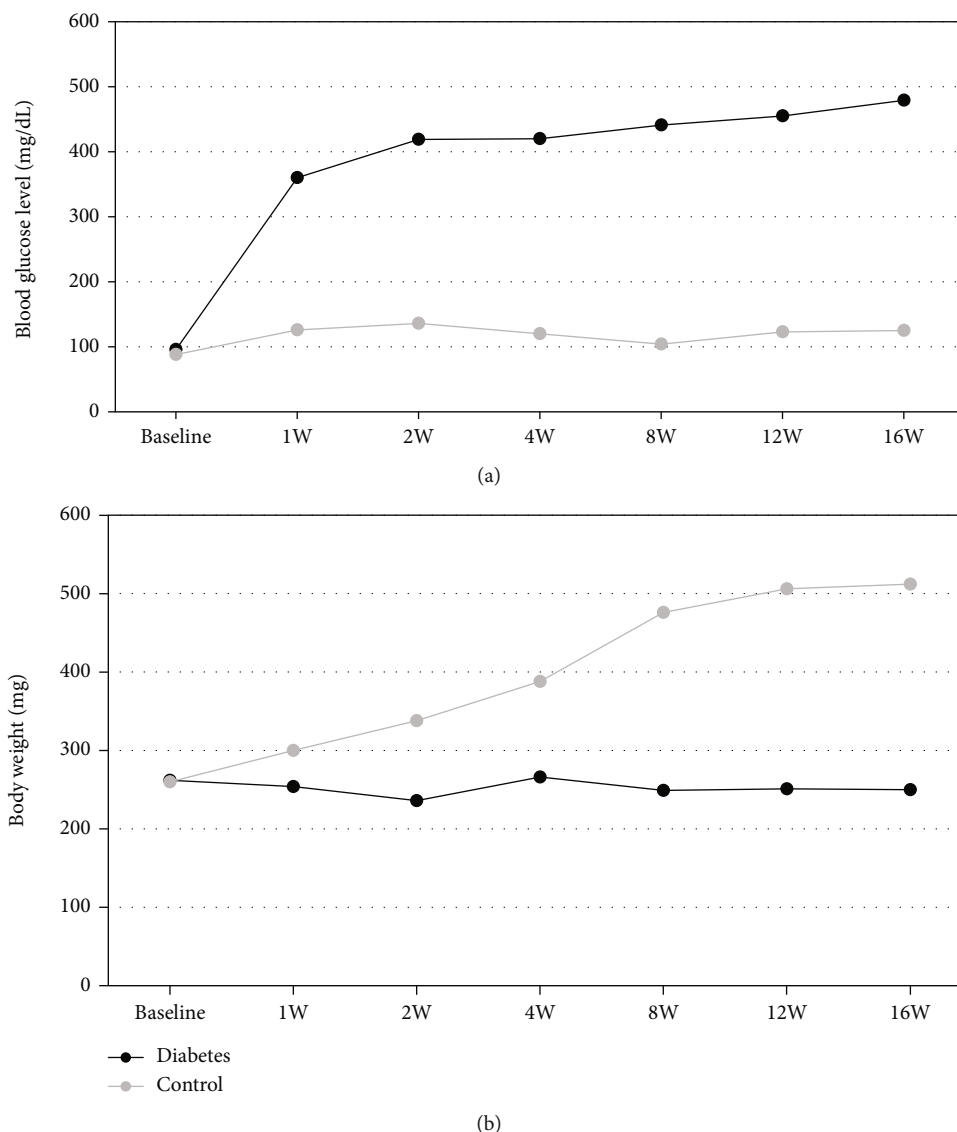
FIGURE 1: (a) Blood glucose levels (mg/dL) and (b) body weight of control and diabetic rats.

3. Results

3.1. Blood Glucose Level and Body Weight of Rats after STZ Injection.
In normal control rats, the blood glucose level remained relatively constant (88 ± 12 mg/dL) for the entire experimental period, and the body weight gradually increased with time (Figure 1). However, in rats injected with STZ, the blood glucose levels increased significantly 1 week after the injection and reached a plateau at 16 weeks (479.6 ± 92.8 mg/dL). At 16 weeks, no significant differences were observed in body weight between STZ-injected rats and controls.

3.2. Microglial Morphology.
Histological analysis of HE-stained sections revealed no significant changes in the retina at early time points. After 8 weeks, mild thinning of the inner layers of the retina was observed (Figure 2). In the control group, Iba-1+ cells were mainly distributed in the inner layers of the retina, and most microglia exhibited a ramified morphology. In the diabetic group, amoeboid morphology was observed in the ganglion cell layer (GCL) and inner plexiform layer (IPL) of the retina, 4 weeks after diabetes onset, with increasing cell number over time. Some microglia, identified as activated microglia, exhibited relatively hypertrophied cell bodies. Activated microglia in the retina of 12- and 16-week diabetic rats presented more hypertrophied cell bodies with coarse processes.

3.3. Microglial Density and Activation.
The density of Iba-1+ retinal microglia significantly increased in diabetic rats compared to control rats at 4-week postdiabetes onset and peaked at 12-week postdiabetes onset ($297.2\% \pm 69.74\%$). This was maintained at a high level at 16-week postdiabetes onset ($178.9\% \pm 83.65\%$) (Figure 3).

Confocal analysis of double-stained tissue sections confirmed that ED1 expression mostly appeared in Iba1+ cell bodies and it was also observed in some processes. While identifying activated microglia, a significant increase in

(a)

(b)

(c)

(d)
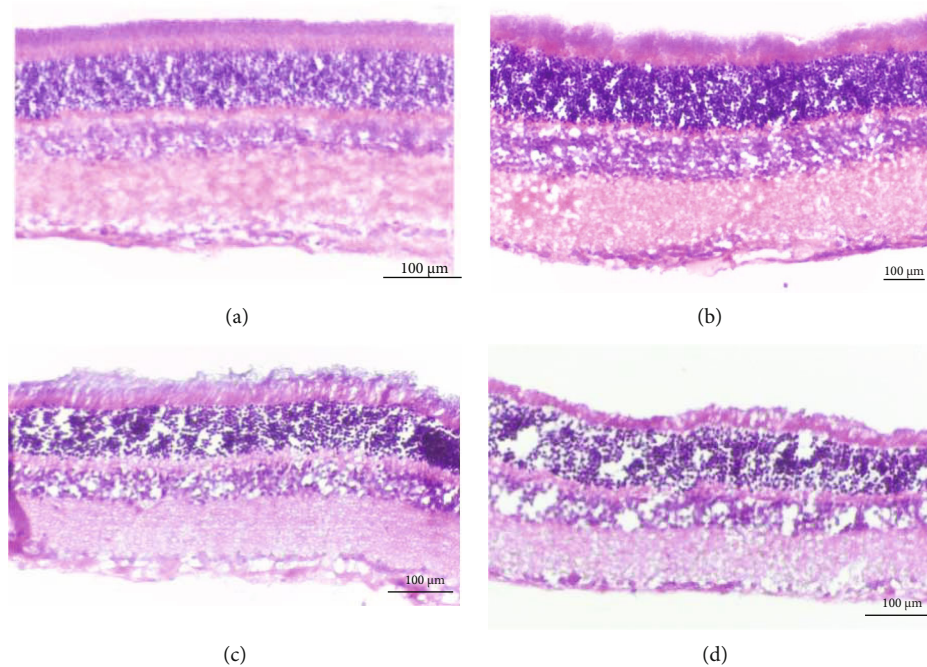
FIGURE 2: Histology of HE-stained sections in diabetic rats: (a) control; (b) 4 weeks; (c) 8 weeks; (d) 16 weeks. After 8 and 16 weeks, mild thinning of the inner layers of the retina was observed.

ED1 expression was detected in the cells exposed to high glucose for 1 week. ED1 expression reached a peak at 4-week postdiabetes onset and remained high in 16-week diabetic rats (Figure 4).

3.4. Microglial Distribution. Microglia in the retinas of control rats were distributed generally in the GCL (25.9% ± 2.47%) and IPL (26.3% ± 1.63%). Moreover, fewer microglia were observed in the outer plexiform layer (OPL), outer nuclear layer (ONL), and rod/cone layer. In 4-week diabetic rats, 45.36 ± 11.42% of microglia were located in the GCL and 20.47 ± 1.34% in the IPL ($p = 0.025$). During this period, the number of microglial cells increased in the GCL, with a concomitant decrease in that in the IPL. However, the distribution of microglial cells changed in the GCL with a simultaneous increase in IPL after 12 and 16 weeks ($p = 0.046$ and $p = 0.012$, respectively) (Figure 5).

3.5. Microglial Proliferation. To determine whether diabetic modeling affects the proliferation of retinal cells, we evaluated the expression of Ki-67, a proliferation cell marker using IHC. In control eyes, weak Ki-67 expression was observed only in the endothelial cells; however, in diabetic rats, weak (but evident) Ki-67 expression was observed mainly in the inner retinal layers. We identified cells that coexpressed Iba-1 and Ki-67, indicating that the active microglial cells (Iba-1+) were also proliferating (Ki-67+) and migrating. The intensity of Iba-1+/Ki-67+ cells increased slightly in 4-week diabetic rats compared to the age-matched control rats ($2.35 ± 0.89$, $p > 0.05$). However, a significant increase was observed in the 12- and 16-week diabetic rats ($3.78 ± 0.54$, $p < 0.05$; $3.48 ± 0.61$, $p < 0.05$, respectively) (Figure 6).

4. Discussion

Recent evidence suggests that the activation and migration of microglial cells may have detrimental and/or beneficial effects on the adjacent neurons. Therefore, it is important to study the mechanisms underlying microglial activation. Insights gained from such studies would enable us to find effective treatment for diseases associated with microglial dysfunction.

Microglial responses to neural damage can be attributed to factors that induce acute neuronal death, recruit peripheral immune cells, and induce the transformation of resident microglia into phagocytic macrophage-like cells. These cells play a pivotal role in the inflammatory processes in the ischemic retina that are normally sequestered from the systemic immune system by the blood–ocular barrier [16, 17].

In human eyes, numerous clusters of hypertrophic microglia can be seen at different stages of DR [18]. A previous study reported microglial activation in the retinas of 4-week diabetic animals, as evidenced by the transition of the microglia from the ramified form to amoeba-shaped form [15, 19]; however, Chen et al. [19] reported that 12-week diabetic rats exhibited a significant increase in the percentage of activated microglia, without any concurrent increase in the microglial density. In the present study, we assessed the microglial responses under proinflammatory conditions in the early stages of STZ-induced diabetes including within 4 weeks.

(a)

(b)
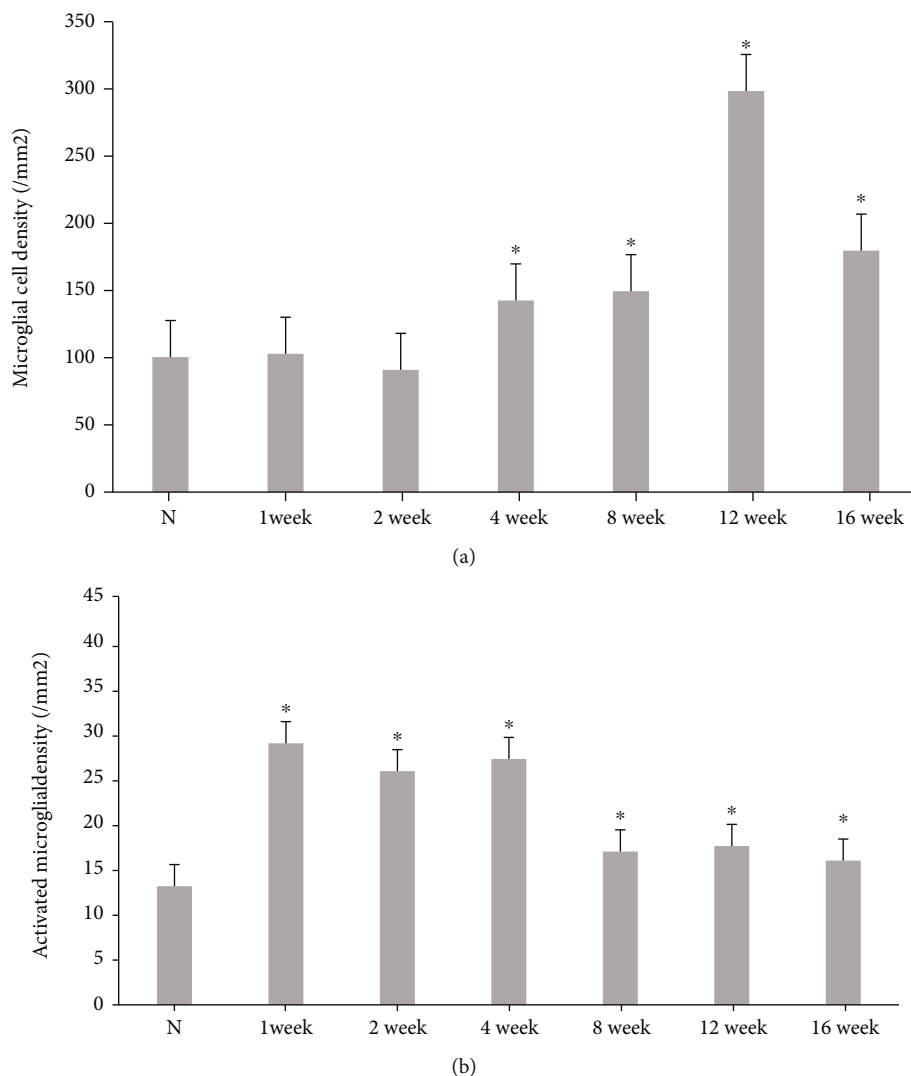
FIGURE 3: Density of total microglia (a) and activated microglia (b) in the retinas of control and diabetic rats. $^*p < 0.05$ versus control.

Iba-1 is a marker of both quiescent and activated microglia. Activated microglia exhibit high Iba-1 expression, enlarged soma, and fewer and shorter processes. In previous studies, Iba-1 was prominently expressed in 4-week diabetes rats, and Iba-1 expression peaked at 12-week postdiabetes onset, indicating a remarkable change in the microglial cells. However, Shi et al. reported that Iba-1 cannot be used on its own to detect active microglia in experimental DR [20]; they suggest that costaining with Iba-1 and other microglial activation markers such as CD11b could accurately reflect the status of microglial activation. Therefore, in the present study, we used ED1 as a marker to evaluate the activation of microglia. IHC revealed that the number of ED1+ cells significantly increased 1 week after diabetes induction; furthermore, activated microglia exhibited hyperplasia and hypertrophy. In our studies, the expression of Iba-1 increased at 4-week postdiabetes onset and peaked at 12 weeks; this result is consistent with that of previous studies [20, 21].

In the present study, although no significant increase in Iba-1 expression was detected, microglial activation—with morphological changes and distribution—was initiated within

1 week of diabetes onset. The majority of microglia was distributed in the inner retina, particularly the IPL, in normal control rats. In experimental diabetic rats, the microglia reacted within 1 week of migratory response. The retinal microglia were redistributed, with higher counts in the GCL and lower counts in the IPL. This change could be relatively attributed to microglial migration, which can be identified under both physiological and pathological conditions [22–24].

In the present study, Iba-1 expression in the retina increased slightly at 4-week postdiabetes onset and reached a significantly higher level at 8- and 12-week postdiabetes onset. The most remarkable change in microglia was detected at 12-week postdiabetes onset; this change was consistent with Ki67 expression. Ki-67 antigen is a well-established marker of proliferating cells. Dual staining for Iba-1 and Ki-67 can enable the detection of active microglia that are proliferating as well. We characterized the proliferating cells in diabetic rats with predominant microglia cells and fewer infiltrating macrophages [25, 26]. The marked increase in the expression of Ki-67 and Iba-1 after the induction of experimental diabetes can presumably be attributed
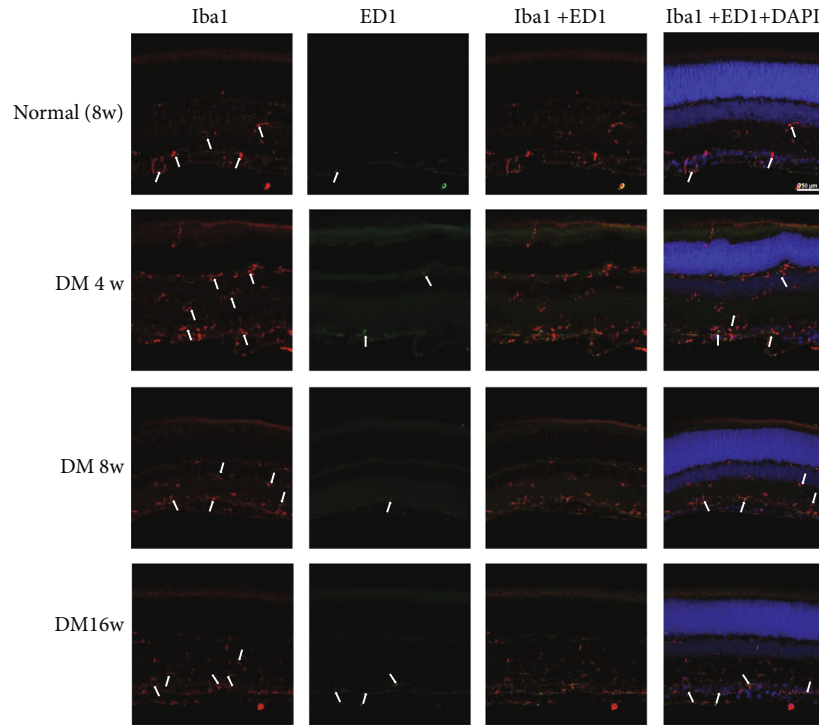
FIGURE 4: Changes in microglia in normal control and experimental diabetic rat retinas. The retinas were immunostained with Iba-1 antibody (red) and ED1 (green). The nuclei were counterstained with DAPI (blue).
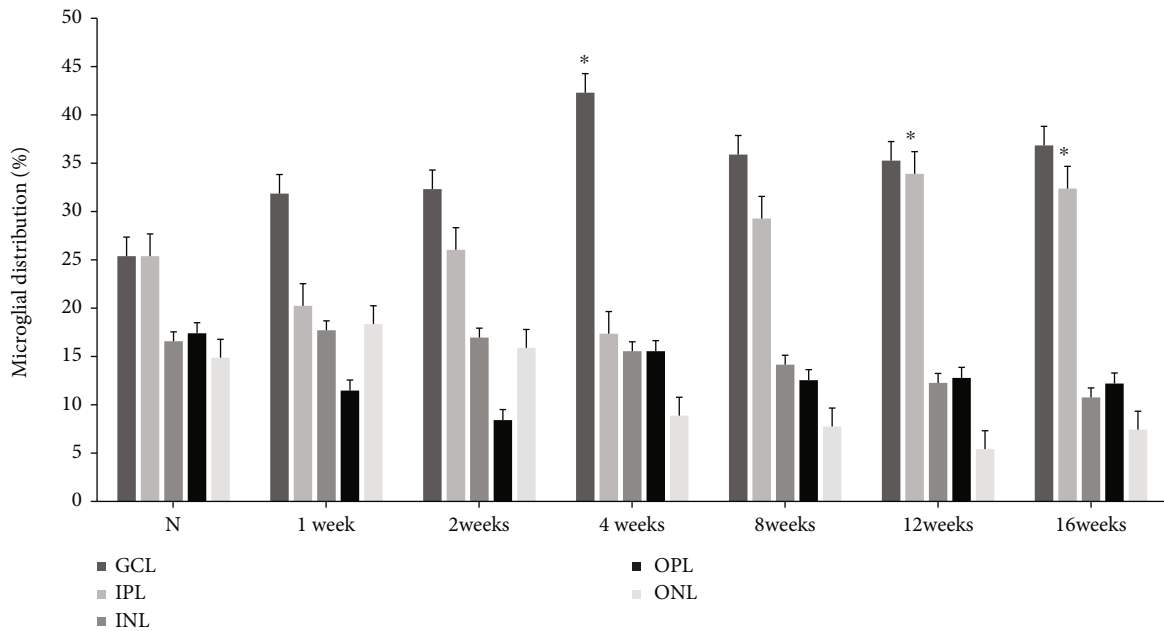
FIGURE 5: Retinal distribution of microglia in the retinas of control and experimental diabetic rats. In the retinas of 12-week diabetic rats, the proportion of microglia increased in the GCL with a concomitant change in the IPL compared with that in other groups. $^{*}p < 0.05$ versus other groups.

to the infiltration or proliferation of nonresident microglia and macrophages. This hypothesis can be further substantiated by the fact that the expression of Ki-67 and Iba-1 was not detectable in the control eyes, even though blood-borne macrophages were visible, thereby indicating subsequent cellular infiltration. Nevertheless, further studies need to address whether increase in the Ki-67 and Iba-1 expression is because of the infiltration of microglial cells into the retina or is it the result of the proliferation of resident microglial cells.
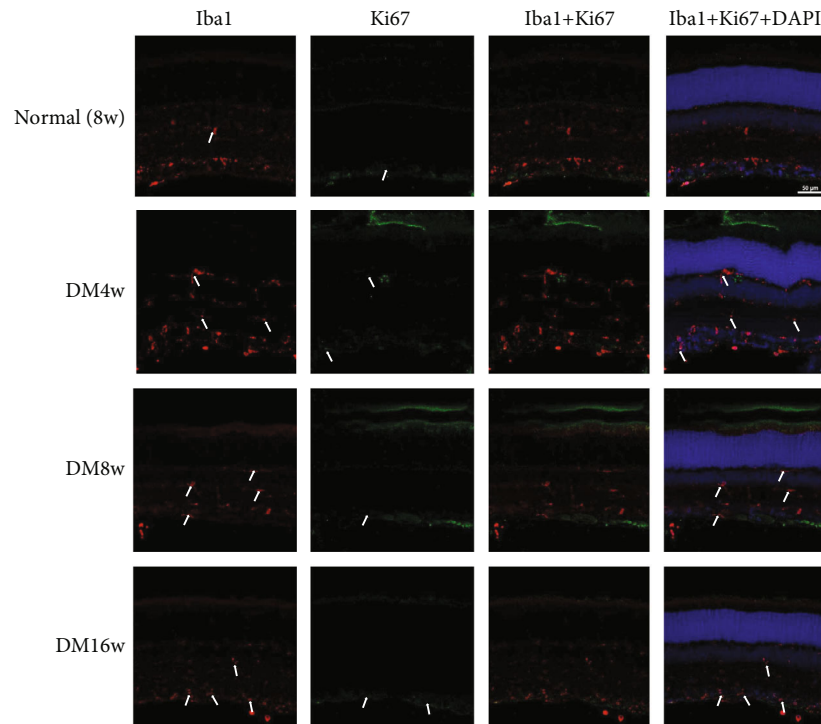
FIGURE 6: Changes in microglia in normal control and experimental diabetic rat retinas. The retina was immunostained with Iba-1 antibody (red) and Ki-67 (green). The nuclei were counterstained with DAPI (blue).

The principle finding from this longitudinal study was that classical microglial activation was initiated within 1 week of diabetes onset. Even if the total amount of microglia activation did not increase, changes in the distribution of microglia were already initiated within 1 week. Moreover, IHC for Iba-1 and ED1 expression confirmed microglial activation during early stages of experimental diabetes in the retina of rats. Upregulation of these molecules after the induction of diabetes in rats coincides with microglial activation that is implicated in various diseases [24, 27].

Although microglial activation has been recognized as a notable neuropathological change in DR, its role in pathogenesis remains to be elucidated. Activated microglia release various proinflammatory chemokines and cytokines, including tumor necrosis factor-α, vascular endothelial growth factor, and interleukin-1β [28–30] In recent studies, minocycline (microglial activation inhibitor) has been employed to explore the role of microglia in different diseases [19, 31]. However, their results could merely be a restrictive effect. More precise research is needed to investigate the function and influence of microglia.

5. Conclusions

Microglia were activated in the retinas of early-stage diabetic rats; changes were observed in microglial morphology, density, and distribution within 1 week of diabetes onset. Early activation of retinal microglia in diabetic rats may be indicative of their importance in DR pathogenesis, which requires further investigation.

Data Availability

The data used to support the findings of this study are available from the corresponding author upon request.

Conflicts of Interest

The authors declare that there is no conflict of interest regarding the publication of this paper.

Acknowledgments

References

[1] M. M. Nentwich and M. W. Ulbig, "Diabetic retinopathy - ocular complications of diabetes mellitus," *World Journal of Diabetes*, vol. 6, no. 3, pp. 489–499, 2015.

[2] S. E. Moss, R. Klein, and B. E. Klein, "The 14-year incidence of visual loss in a diabetic population[1]," *Ophthalmology*, vol. 105, no. 6, pp. 998–1003, 1998.

[3] F. Lazzara, A. Fidilio, C. B. M. Platania et al., "Aflibercept regulates retinal inflammation elicited by high glucose _via_ the PlGF/ERK pathway," *Biochemical Pharmacology*, vol. 168, pp. 341–351, 2019.

[4] C. H. Meyer, "Current treatment approaches in diabetic macular edema," *Ophthalmologica*, vol. 221, no. 2, pp. 118–131, 2007.

[5] G. Giurdanella, C. D. Anfuso, M. Olivieri et al., "Aflibercept, bevacizumab and ranibizumab prevent glucose-induced damage in human retinal pericytes _in vitro_ , through a PLA$_2$/COX-2/VEGF-A pathway," Biochemical Pharmacology, vol. 96, no. 3, pp. 278–287, 2015.

[6] F. Lazzara, M. C. Trotta, C. B. M. Platania et al., "Stabilization of HIF-1α in human retinal endothelial cells modulates expression of miRNAs and proangiogenic growth factors," Frontiers in Pharmacology, vol. 11, p. 1063, 2020.

[7] C. B. M. Platania, R. Maisto, M. C. Trotta et al., "Retinal and circulating miRNA expression patterns in diabetic retinopathy: an in silico and in vivo approach," British Journal of Pharmacology, vol. 176, no. 13, pp. 2179–2194, 2019.

[8] T. S. Kern, "Contributions of inflammatory processes to the development of the early stages of diabetic retinopathy," Experimental Diabetes Research, vol. 2007, Article ID 95103, 14 pages, 2007.

[9] E. L. Fletcher, J. A. Phipps, and J. L. Wilkinson-Berka, "Dysfunction of retinal neurons and glia during diabetes," Clinical & Experimental Optometry, vol. 88, no. 3, pp. 132–145, 2005.

[10] T. Zhang, X. Mei, H. Ouyang et al., "Natural flavonoid galangin alleviates microglia-trigged blood-retinal barrier dysfunction during the development of diabetic retinopathy," The Journal of Nutritional Biochemistry, vol. 65, pp. 1–14, 2019.

[11] S. Ahmad, N. M. ElSherbiny, M. S. Jamal et al., "Anti-inflammatory role of sesamin in STZ induced mice model of diabetic retinopathy," Journal of Neuroimmunology, vol. 295-296, pp. 47–53, 2016.

[12] X. Y. Mei, L. Y. Zhou, T. Y. Zhang, B. Lu, and L. L. Ji, "<i>Scutellaria barbata</i> attenuates diabetic retinopathy by preventing retinal inflammation and the decreased expression of tight junction protein," International Journal of Ophthalmology, vol. 10, no. 6, pp. 870–877, 2017.

[13] H. Ouyang, X. Mei, T. Zhang, B. Lu, and L. Ji, "Ursodeoxycholic acid ameliorates diabetic retinopathy via reducing retinal inflammation and reversing the breakdown of blood-retinal barrier," European Journal of Pharmacology, vol. 840, pp. 20–27, 2018.

[14] X. Mei, T. Zhang, H. Ouyang, B. Lu, Z. Wang, and L. Ji, "Scutellarin alleviates blood-retina-barrier oxidative stress injury initiated by activated microglia cells during the development of diabetic retinopathy," Biochemical Pharmacology, vol. 159, pp. 82–95, 2019.

[15] X. X. Zeng, Y. K. Ng, and E. A. Ling, "Neuronal and microglial response in the retina of streptozotocin-induced diabetic rats," Visual Neuroscience, vol. 17, no. 3, pp. 463–471, 2000.

[16] C. Kaur, W. S. Foulds, and E. A. Ling, "Blood-retinal barrier in hypoxic ischaemic conditions: basic concepts, clinical features and management," Progress in Retinal and Eye Research, vol. 27, no. 6, pp. 622–647, 2008.

[17] J. V. Forrester, H. Xu, L. Kuffova, A. D. Dick, and P. G. McMenamin, "Dendritic cell physiology and function in the eye," Immunological Reviews, vol. 234, no. 1, pp. 282–304, 2010.

[18] H. Y. Zeng, W. R. Green, and M. O. Tso, "Microglial activation in human diabetic retinopathy," Archives of Ophthalmology, vol. 126, no. 2, pp. 227–232, 2008.

[19] J. K. Krady, A. Basu, C. M. Allen et al., "Minocycline reduces proinflammatory cytokine expression, microglial activation, and caspase-3 activation in a rodent model of diabetic retinopathy," Diabetes, vol. 54, no. 5, pp. 1559–1565, 2005.

[20] F. J. Shi, C. Y. Zhang, H. F. Qin et al., "Is Iba-1 protein expression a sensitive marker for microglia activation in experimental diabetic retinopathy?," International Journal of Ophthalmology, vol. 14, no. 2, pp. 200–208, 2021.

[21] X. Chen, H. Zhou, Y. Gong, S. Wei, and M. Zhang, "Early spatiotemporal characterization of microglial activation in the retinas of rats with streptozotocin-induced diabetes," Graefe's Archive for Clinical and Experimental Ophthalmology, vol. 253, no. 4, pp. 519–525, 2015.

[22] K. Ohsawa and S. Kohsaka, "Dynamic motility of microglia: purinergic modulation of microglial movement in the normal and pathological brain," Glia, vol. 59, no. 12, pp. 1793–1799, 2011.

[23] E. Rungger-Brandle, A. A. Dosso, and P. M. Leuenberger, "Glial reactivity, an early feature of diabetic retinopathy," Investigative Ophthalmology & Visual Science, vol. 41, no. 7, pp. 1971–1980, 2000.

[24] A. S. Ibrahim, A. B. el-Remessy, S. Matragoon et al., "Retinal microglial activation and inflammation induced by Amadori-glycated albumin in a rat model of diabetes," Diabetes, vol. 60, no. 4, pp. 1122–1133, 2011.

[25] R. Naskar, M. Wissing, and S. Thanos, "Detection of early neuron degeneration and accompanying microglial responses in the retina of a rat model of glaucoma," Investigative Ophthalmology & Visual Science, vol. 43, no. 9, pp. 2962–2968, 2002.

[26] H. Kaneko, K. M. Nishiguchi, M. Nakamura, S. Kachi, and H. Terasaki, "Characteristics of bone marrow-derived microglia in the normal and injured retina," Investigative Ophthalmology & Visual Science, vol. 49, no. 9, pp. 4162–4168, 2008.

[27] N. Schallner, M. Fuchs, C. I. Schwer et al., "Postconditioning with inhaled carbon monoxide counteracts apoptosis and neuroinflammation in the ischemic rat retina," PLoS One, vol. 7, no. 9, article e46479, 2012.

[28] N. Demircan, B. G. Safran, M. Soylu, A. A. Ozcan, and S. Sizmaz, "Determination of vitreous interleukin-1 (IL-1) and tumour necrosis factor (TNF) levels in proliferative diabetic retinopathy," Eye (London, England), vol. 20, no. 12, pp. 1366–1369, 2006.

[29] A. Kroner, A. D. Greenhalgh, J. G. Zarruk, R. Passos Dos Santos, M. Gaestel, and S. David, "TNF and increased intracellular iron alter macrophage polarization to a detrimental M1 phenotype in the injured spinal cord," Neuron, vol. 83, no. 5, pp. 1098–1116, 2014.

[30] M. Marone, G. Scambia, G. Bonanno et al., "Transforming growth factor-β1 transcriptionally activates CD34 and prevents induced differentiation of TF-1 cells in the absence of any cell-cycle effects," Leukemia, vol. 16, no. 1, pp. 94–105, 2002.

[31] A. Wang, A. Yu, L. Lau et al., "Minocycline inhibits LPS-induced retinal microglia activation," Neurochemistry International, vol. 47, no. 1-2, pp. 152–158, 2005.

Research Article

Ellipsoid Zone Integrity and Visual Acuity Changes during Diabetic Macular Edema Therapy: A Longitudinal Study

Lucy J. Kessler [ID],[1,2] **Gerd U. Auffarth,**[1] **Dmitrii Bagautdinov,**[1] **and Ramin Khoramnia**[1,2]

[1]*Department of Ophthalmology, University of Heidelberg, Heidelberg 69120, Germany*
[2]*HEiKA–Heidelberg Karlsruhe Strategic Partnership, Heidelberg University and Karlsruhe Institute of Technology (KIT),*
 Karlsruhe 76131, Germany

Correspondence should be addressed to Lucy J. Kessler; lucyjoanne.kessler@med.uni-heidelberg.de

Received 6 August 2021; Accepted 6 September 2021; Published 7 October 2021

Academic Editor: Maria Vittoria Cicinelli

Purpose. Ellipsoid zone (EZ) integrity is identified as a potential biomarker for therapy surveillance and outcome prediction of visual acuity (VA). However, only a few studies report long-term results of over 1 year of clinical and anatomical changes in patients with diabetic macular edema (DME). This study is aimed at describing the long-term VA and anatomical outcomes in spectral domain optical coherence tomography (OCT) (relative ellipsoid zone reflectivity ratio, central macular thickness, and volume) in patients with DME treated with antivascular endothelial growth factor (anti-VEGF) therapy. Furthermore, we studied the correlation between EZ integrity and changes in visual acuity. *Methods*. 71 eyes of 71 patients were included in this retrospective study. Clinical characteristics were reviewed yearly. OCT data were assessed at baseline and after 1, 3, and 5 years. EZ parameters were quantified automatically. OCT parameters and visual outcome were correlated and analyzed in multivariable regression models. *Results*. EZ reflectivity ratio correlated with functional outcome in DME patients from baseline to fifth year at all time points (for all $p < 0.05$). EZ reflectivity improved the most in the first year of treatment (0.68 to 0.75; $p < 0.05$) and declined gradually until year 5 of therapy (0.71; compared to baseline $p > 0.05$). Similarly, best VA was achieved after 1 year (0.40 logarithm of the minimum angle of resolution (logMAR) to 0.28 logMAR; $p < 0.001$) and declined gradually until year 5. Final VA in year 5 was comparable to baseline (0.45 logMAR, compared to baseline $p > 0.05$). Together with baseline VA, baseline EZ parameters did predict VA outcome after 1 year ($p < 0.05$). Concordantly, VA and EZ parameters from year 1 were associated with VA outcome in year 2. *Conclusion*. This study described the long-term course of EZ changes during anti-VEGF treatment in DME patients. In addition, our results underlined the potential of EZ parameters as novel OCT biomarkers for prediction of VA outcomes during therapy.

1. Introduction

Center involved diabetic macular edema (DME) is a sight threatening manifestation in patients with diabetic retinopathy [1–3]. Intravitreal antivascular endothelial growth factor (anti-VEGF) injection has become the standard of care in preventing further vision loss [4, 5]. Response to anti-VEGF treatment is evaluated by clinical and morphological parameters in optical coherence tomography (OCT) [6, 7]. To date, it has been difficult to determine individual response, disease activity, and potential visual preservation over time. In the past, OCT parameters in clinical settings have been limited to "global" measurements of retinal thick-

ness and macular volume. From recent research, it appears that novel OCT biomarkers can be used to better understand individual therapy response, disease progression, and improve treatment [8] One of these emerging OCT biomarkers is the relative ellipsoid zone reflectivity ratio (EZR) [9]. In healthy eyes, the external limiting membrane (ELM), ellipsoid zone (EZ), and retinal pigment epithelium (RPE) are represented in OCT as hyperreflective bands. EZ is defined as the hyperreflective band posterior to the ELM, and its hyperreflectivity is assumed due to high mitochondrial density in the inner segments of photoreceptor cells, indicating the vitality of these photoreceptors [9]. Changes of optical reflectivity of EZ have been observed in retinal

pathologies [10–12]. Previous studies demonstrated a correlation of recovery of ellipsoid zone and visual acuity in retinal diseases [10, 13–17]. In diabetic macular edema, sequential restoration of EZ was observed after one year of anti-VEGF treatment [18]. However, the long-term outcome of EZR during anti-VEGF treatment remains unknown. Additionally, in several studies, the quantitative analysis of EZR was laborious and time consuming as the measurements were manually obtained and mostly at a limited number of regions of interest [16, 19, 20]. The aim of this study is to evaluate the ellipsoid zone outcome (EZR and EZ-RPE distance) during a 3- to 5-year follow-up of DME patients under anti-VEGF therapy and to find potential correlation with the visual acuity outcome beyond 1 year after treatment initiation. Our analysis of the EZ characteristics was greatly facilitated by an automated quantitative examination of 27 regions of interest of fovea-centered OCT B-scan at each time point. The evaluation is therefore objective and comprises 4833 measurements in total.

2. Materials and Methods

This was a retrospective study conducted at the University Eye Hospital of Heidelberg, Germany. Local ethics committee approval was obtained from the University of Heidelberg. All study protocols adhered to the tenets of the Declaration of Helsinki. This study was registered on the German Clinical Trial Register (registration number: DRKS00024399).

2.1. Study Cohort. We reviewed patients with treatment-naive DME who began anti-VEGF therapy between 2010 and 2018 with a minimum of 3-year follow-up period at our hospital. 5-year data was available from 37 out of 71 patients. VA was assessed yearly. OCT parameters were quantified at baseline and years 1, 3, and 5. These time points were chosen because several real-world studies with long-term follow up in patients with DME showed that most VA gain and structural changes were noticed at year 1, but VA worsening was observed after 3 years [21–23]. Therefore, evaluating OCT parameters changes at third year may provide more insight in the changes of structural OCT between the year 1 and year 5.

Exclusion criteria included age younger than 18 years, retinal or glaucoma surgery before the first anti-VEGF injection, amblyopia, uveitis, and uncontrolled glaucoma. Presence of other retinal diseases associated with macular edema such as retinal venous or arterial occlusive disease, severe epiretinal membrane, alterations of outer retinal layers, like drusen, pigment epithelium detachment, and EZ atrophy due to age-related macular degeneration also led to exclusion. Refractive error of more than 6 diopter spherical equivalents, lack of OCT-scans at any time point, or OCT imaging of low quality or signal strength (<30/35 with 35/35 being the best signal to noise ratio) that impaired analysis were excluded. Patients who received anti-VEGF injections in other clinics were excluded as well. If both eyes were eligible for study inclusion, as study eye, we chose the eye with the worse best corrected visual acuity at baseline.

Treatment initiation was our baseline point when patients began to receive monthly intravitreal anti-VEGF injections (ranibizumab, aflibercept, or offlabel bevacizumab). This was followed by retreatment on the basis of treat and extend regimen at the discretion of the treating ophthalmologist. The treatment decision was derived from the German or European guideline for treatment that was valid at that time [6, 24–26]. In the past, treat and extend regimen has been continuously modified due to new findings or in the attempt to further reduce injection burden. Some changes in injection scheme also applied to our study population from 2010 to 2018. For example, as early as 2010, injection intervals were extended or shortened in a fixed 2-week scheme. However, we subsequently also allowed a shortening or extension of interval of only 1 week in cases when overall treatment response was difficult to determine to allow a closer observation of disease activity. Therefore, we compared baseline statistics of the 3-year and 5-year cohorts to confirm nonsignificant differences despite of different follow-up times. 31 patients received additional dexamethasone implants during therapy. All patients underwent a comprehensive ophthalmologic examination at each visit, which included measurement of the best-corrected visual acuity (BCVA), slit-lamp biomicroscopy, indirect funduscopy, and spectral domain OCT (Spectralis, Heidelberg Engineering, Heidelberg, Germany). At each visit, we obtained the patient's latest HbA1c serum level.

2.2. Optical Coherence Tomography Acquisition and Analysis

2.2.1. Image Acquisition. Images were obtained at each visit using the Spectralis Spectral Domain OCT with HeyEx software, versions 5.3.0.7 to 6.3.2.0 (Heidelberg Engineering GmbH, Heidelberg, Germany). We used a 6 mm × 6 mm macular cube line scan protocol to obtain the image data. The scan recorded at baseline was set as reference to ensure all subsequent OCT scans were acquired at precisely this location. The horizontal B-scan through the foveola was extracted for further analysis. All scans were applied in high-resolution mode (512 pixels along the x-axis) and an automated averaging of 9 frames for each line scan. Central macular thickness (CMT) and macular volume (MV) were obtained from device-integrated software.

2.2.2. Image Processing and Analysis. Logarithmic-transformed display of OCT was exported as tagged image file format (TIFF) using the integrated Heidelberg Eye Explorer Software, version 1.10.4.0 (Heidelberg Engineering GmbH, Heidelberg, Germany). Prior to image analysis, image registration and signal normalization were applied using Fiji software, version 2.1.0/1.53c (US National Institutes of Health, Bethesda, US. https://imagej.net/software/fiji/) [27]. The foveola was used as center landmark for rigid image registration. OCT image with least speckle noise and best contrast was used as reference for histogram matching to normalize all OCT images. Longitudinal reflectance profile was obtained at every 200 μm, thus resulting in 27 measurements of each OCT scan. The width of each region of interest (ROI) was set at 4 pixels (approximately 44 μm). Reflectance

Overview of regions of interest on B-scan

Representative longitudinal reflectance profile

(a) Overview of regions of interest on B-scan

(b) Representative longitudinal reflectance profile
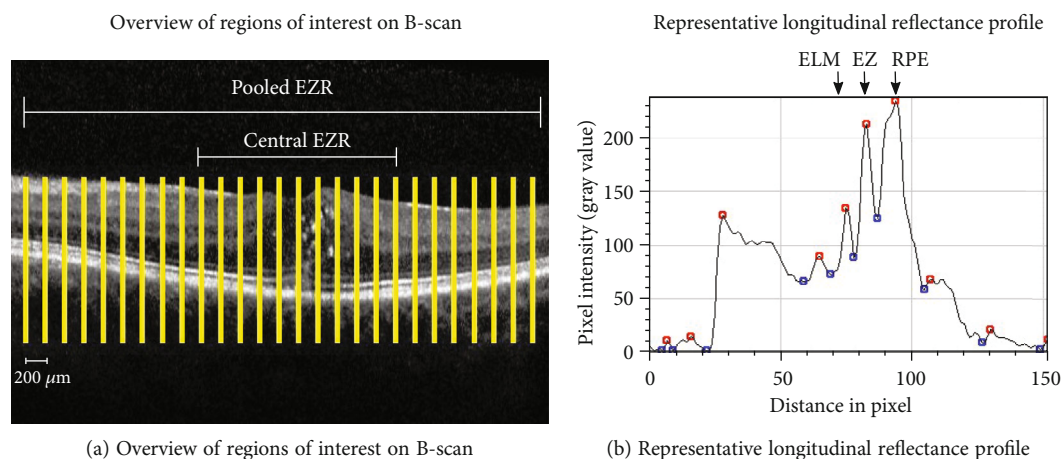
FIGURE 1: (a) Overview of regions of interest (ROI). In total, 27 measurements in 200 μm distance of each OCT B-scan were obtained and analyzed. (b) shows a representative longitudinal reflectance profile at each ROI. Pixel intensity values ranged from 0 (black) to 255 (white) on gray scale. Maxima values ("peaks") are represented by red dots and minima values between the peaks that are represented by blue dots.

profiles were taken in an automated fashion using a customized script including plot profile extraction in Fiji. This approach has been described elsewhere as a robust method to access EZ integrity [11, 19, 20]. Manual adjustment was not applied. Coordinates of peak values of the reflectance profile were stored as numeric values in a Microsoft Excel file (Microsoft Corp., Redmond WA, USA). Before retrieving and averaging peak values, plausibility of designated peak values was ensured by comparing plot profile and genuine OCT images. In reflectance profile, retinal pigment epithelium (RPE) is considered as the last hyperreflective band in the outer retina, whereas the ellipsoid zone (EZ) is the second hyperreflective band following the external limiting membrane (ELM). Relative ellipsoid zone reflectivity (EZR) was calculated as the ratio of EZ reflectivity to RPE reflectivity. The average value of EZR of the central 2000 μm (in total 10 measurements) was considered as central EZR (c-EZR), and the average of all measurements (in total 27 measurements) was considered as pooled EZR (p-EZR) (Figure 1(a)). By averaging 27 measurements, shadowing effects caused by local pathologies such as hyperreflective dots or vessels that affect the optical reflectivity of underlying structures were mitigated. Only peak distance between EZ and RPE optical density more than 2 pixels (~22 μm) was considered as two distinct peaks. Any peak distance below that was considered a partial EZ attenuation or atrophy was therefore not counted as a peak value and thus was not counted into the averaging calculation (Figure 1(b)). These thresholds were chosen according to the existing literature [28, 29].

2.3. Statistical Analysis. Snellen visual acuity was converted to logMAR for statistical analysis. For descriptive analysis, categorical data are presented as frequency and percentage (n; %); continuous data are shown as means with standard deviations (SD), median, and first and third quartile. Pearson's chi^2 test and Mann–Whitney U test were applied to test for differences between independent groups. Spearman's

Rho (ρ) was used for correlation analysis. For variance analysis, the Friedman test was applied to test for differences of continuous parameters across follow-up time points. Multiple variable linear regression analyses were performed to evaluate the effect of baseline parameters and mean changes between baseline and 1 year on visual outcome after 1 and 2 years, respectively. Multicollinearity, intercorrelation between independent variables that potentially can lead to model overfitting, was evaluated with variation inflation factor testing, and no models were run with variation inflation factor over 3 for any prediction. Statistical analysis was performed in IBM SPSS Statistics software version 27.0 (IBM Corp., Armonk, NY, USA); two-sided $p < 0.05$ was considered as statistically significant.

3. Results

3.1. Study Population. The mean age of the entire cohort was 59 (range: 42-79 years). In total, 45 patients were male (63.40%). 5-year data was available from 37 of 71 patients (71 eyes) (52%). At presentation, all eyes received the first intravitreal injection of one of three anti-VEGF medications: 74.60% got bevacizumab as first injection, 19.70% got ranibizumab, and 5.60% received aflibercept. During the observation period, between 2010 and 2018, the treatment guidelines were occasionally updated. Therefore, we compared the baseline characteristics of patients with and without 5-year data to confirm that both subgroups were comparable at baseline despite the difference in follow-up time (Table 1). There was no significant difference in the distribution of sex, age, and HbA1c serum level in both cohorts ($p > 0.05$). The number of patients who received laser treatment (focal or panretinal laser coagulation) prior to first injection and patients with pseudophakic study eyes was similar in both groups ($p > 0.05$). In the first year, the 3-year group received on average two more injections than the 5-year group (5-year group mean: 4.97; 3-year group: 7.00; $p = 0.004$). However,

TABLE 1: Demographics and characteristics for patients with 5-year data ($n = 37$) compared to patients with only 3 years of follow-up ($n = 34$).

Baseline variables	With 5-year data ($n = 37$)		Only 3-year data ($n = 34$)		p
	Mean (SD)	Median (Q1; Q3)	Mean (SD)	Median (Q1; Q3)	
Age (years)	57.54 (8.04)	57.00 (51.00; 63.00)	61.67 (8.80)	63.00 (54.00; 68.00)	0.051°
HbA1c (%)	7.19 (1.27)	6.95 (6.49; 7.88)	7.40 (0.96)	7.37 (6.76; 7.60)	0.886°
VA in logMAR at baseline	0.39 (0.29)	0.30 (0.15; 0.59)	0.42 (0.37)	0.37 (0.10; 0.58)	0.799°
Pooled EZ-RPE reflectivity ratio (arbitrary unit)	0.69 (0.17)	0.70 (0.59; 0.81)	0.67 (0.16)	0.68 (0.59; 0.81)	0.756°
Pooled EZ-RPE distance (in pixel)	11.24 (1.53)	11.04 (9.89; 12.27)	11.33 (3.43)	10,81 (10.07; 11.63)	0.475°
Central retina thickness (in μm)	409.86 (133.22)	367.00 (312.00; 470.00)	419.30 (121.96)	370.50 (321.75; 489.75)	0.600°
Central macular volume (in μm^3)	10.55 (2.19)	9.93 (9.18; 11.53)	10.50 (1.70)	10.39 (9.10; 11.20)	0.756°
	n (%)		n (%)		
Male sex	26 (70.30)		19 (55.90)		0.229†
Laser treatment before treatment	15 (40.54)		9 (26.47)		0.315†
Pseudophakia before treatment	7 (18.91)		12 (35.29)		0.180†
Variables during observation					
Received dexamethasone implants	1.51 (2.90)	0.00 (0.00; 2.00)	1.62 (2.13)	0.50 (0.00; 3.00)	0.444°
Injections per year	5.11 (1.67)	5.08 (3.83; 6.20)	5.83 (1.75)	5.70 (4.27; 6.94)	0.777°
Injections in first year	4.97 (2.35)	5 (3.00; 6.00)	7.00 (2.88)	6.00 (5.00; 10.00)	*0.004°*

logMAR: logarithm of the minimum angle of resolution; p-EZR: pooled relative ellipsoid zone reflectivity; c-EZR: central relative ellipsoid zone reflectivity; EZ: ellipsoid zone; RPE: retinal pigment epithelium; SD: standard deviation; Q1: first quartile; Q3: third quartile. p values from °Mann–Whitney U test and †Pearson's chi^2 test. Values in italic front style denote statistical significance at the $p < 0.05$ level.

injection frequency per year was not significantly different in both groups. During observation time, the number of received dexamethasone implants was not significantly different in both groups ($p > 0.05$). Overall, baseline characteristics were similar in both groups.

3.2. Visual Acuity, Central Retinal Thickness (CRT), and Central Macular Volume.

VA was assessed yearly. OCT parameters including EZR and EZ-RPE distance, central macular thickness, and macular volume were retrieved at the start of treatment and after 1, 3, and 5 years. Changes of VA from treatment initiation to fifth year for the entire cohort are shown in Figure 2. Mean VA improved significantly from 0.40 logMAR (SD: 0.33) at baseline to 0.28 log-MAR after 1 year (SD: 0.27; $p < 0.001$). The improvement was maintained until year 3. After 4 and 5 years, mean VA declined to 0.44 logMAR (SD: 0.30) and 0.45 logMAR (SD: 0.32), which was comparable to baseline VA (for 4 and 5 years: $p > 0.05$ compared to baseline). Figure 3(a) represents the mean changes in CRT. Reduction of CRT was significant for all follow-up time points compared to baseline (for all time points: $p < 0.05$). Overall, CRT was reduced by approximately 46μm after 1 year compared to baseline (from 414μm (SD: 127.12) to 368μm (SD: 132.96), $p < 0.05$). CRT reduced continuously until year 5 to 297μm (SD: 88.15; $p < 0.05$). Mean central macular volume was 10.52μm^3 at baseline and significantly decreased at 1- (9.84μm^3; SD: 2.19; $p < 0.001$) and 3-year follow-up (9.33μm^3; SD: 1.79; $p < 0.001$). Mean central macular volume at year 5 was 8.66μm^3 and was significantly lower than at baseline ($p < 0.001$) (Figure 3(b)).
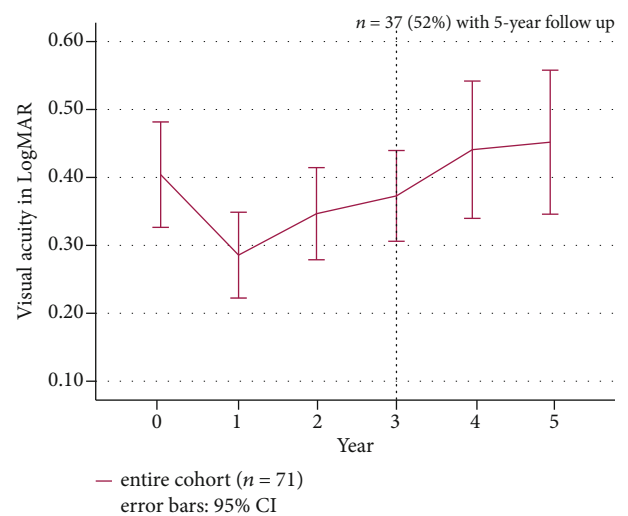
FIGURE 2: Mean visual acuity changes in logMAR from baseline to fifth year. Purple line represents the entire cohort ($n = 71$ until year 3). 4-year and 5-year data were available from 37 patients (dotted line). The 95% confidence interval is shown as error bars. Mean VA improved most in the first year. Improved mean VA was maintained until year 3. After 4 years, mean VA was worse than baseline VA despite continued therapy.

3.3. EZ-RPE Reflectivity Ratio and EZ-RPE Distance.

Following initiation of anti-VEGF therapy, mean p-EZR improved from 0.68 (SD: 0.17) to 0.75 (SD: 0.15) in the first year ($p < 0.001$) and declined gradually to 0.71 (SD: 0.17) after 5 years (compared to baseline: $p > 0.05$) (Figure 3(c)). Mean

(a)

(b)

(c)

(d)

(e)

(f)
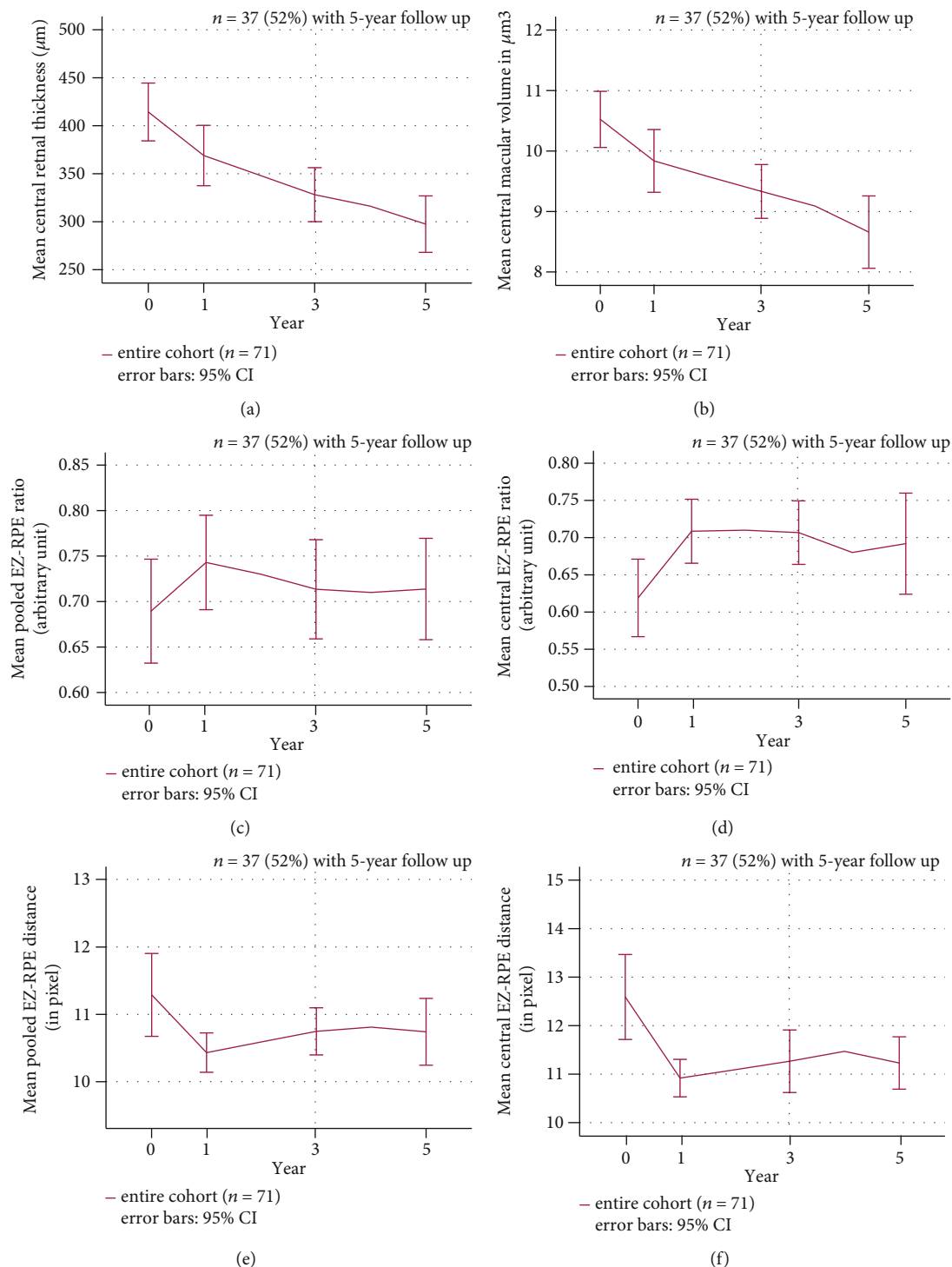
FIGURE 3: Longitudinal changes of OCT parameters from baseline to fifth year. Purple line represents the entire cohort ($n = 71$ until year 3). The 95% confidence interval is represented by error bars. (a) Central retinal thickness and (b) central macular volume decreased significantly during continuous therapy ($p < 0.05$). (c, d) show mean pooled and central EZ-RPE reflectivity ratio changes. (e, f) demonstrate mean pooled and central EZ-RPE distances.

c-EZR improved from 0.62 at baseline (SD: 0.22) to 0.71 (SD: 0.18) in year 1 for the entire cohort ($p < 0.001$). The improvement of c-EZR was maintained at year 3 (0.71, SD: 0.18) and declined in year 5 (0.69, SD: 0.20) after initiation of therapy. c-EZR at all time points was significantly higher than at baseline (for all time points $p < 0.05$) (Figure 3(d)). Baseline pooled EZ-RPE distance significantly reduced during therapy from 11.29 pixel (SD: 2.60) at baseline to 10.43 (SD: 1.24) at year 1 ($p < 0.01$) and 10.74 (SD: 1.49) at year 5 ($p \leq 0.01$) (Figure 3(e)). Baseline central EZ-RPE distance

TABLE 2: Correlation analysis of visual acuity and OCT parameters at baseline, 1, 3, and 5 years. Spearman's correlation coefficient ρ between visual acuity and OCT parameter at each time point is shown. $^*p < 0.05$; $^{**}p < 0.01$; $^{***}p < 0.001$.

| | | Visual acuity | | | |
		Baseline	Year 1	Year 3	Year 5
Pooled EZR	Baseline	-0.52***			
	Year 1		-0.56***		
	Year 3			-0.52***	
	Year 5				-0.59***
Central EZR	Baseline	-0.52***			
	Year 1		-0.65***		
	Year 3			-0.56***	
	Year 5				-0.55***
Pooled EZ-RPE distance	Baseline	0.25*			
	Year 1		0.26***		
	Year 3			0.31*	
	Year 5				0.24
Central EZ-RPE distance	Baseline	0.28*			
	Year 1		0.23		
	Year 3			0.26*	
	Year 5				0.27

reduced from 12.60 pixel (SD: 3.70) to 10.91 (SD: 1.63) after 1 year ($p < 0.01$), 11.00 (SD: 2.72) in year 3 ($p < 0.05$), and 10.91 (SD: 1.62) in year 5 ($p < 0.05$) (Figure 3(f)).

3.4. Correlation and Regression Analysis. At all time points, VA was significantly correlated to p-EZR (ρ ranged from -0.52 to -0.59, $p < 0.05$ at all time points). Correlation of c-EZR to VA was moderately higher than the p-EZR in the first and third year (ρ ranged from -0.52 to -0.65, $p < 0.05$ at all time points). Compared to EZR, pooled and central EZ-RPE distance showed lower yet significant correlation to VA at baseline and third year (Table 2). Mean VA improvement from baseline to year 3 was significantly correlated with improvement of c-EZR ($\rho = −0.31$, $p < 0.01$), central EZ-RPE distance ($\rho = 0.26$, $p < 0.05$), reduction of central retinal thickness ($\rho = 0.40$, $p = 0.003$), and improvement of macular volume ($\rho = 0.40$, $p \leq 0.001$). Analysis with 5-year data revealed significant correlation between changes of VA, pooled, and central EZR after 5 years compared to baseline ($\rho = −0.41$ to -0.44, $p < 0.05$). c-EZR was best correlated to VA change. Correlation to VA change was not significant for mean change of EZ-RPE distance and mean macular volume changes ($p > 0.05$) (Table 3).

Regression models were controlled for age at treatment initiation, injection frequency in the first year, and baseline VA, which correlated strongly to VA improvements at all follow-up time points ($p < 0.001$). Mean change of EZ parameters was tested separately due to multicollinearity to predict change in VA at 1 year. Baseline pooled ($R^2 = 0.52$, $p < 0.001$) and central EZR ($R^2 = 0.51$, $p < 0.001$) as well as pooled ($R^2 = 0.52$, $p < 0.001$) and central ($R^2 = 0.53$, $p < 0.001$) EZ-RPE distance predicted change in VA after 12 months when controlled for the abovementioned variables.

TABLE 3: Correlation analysis of changes in visual acuity and OCT parameters between baseline to third year and baseline to fifth year. Spearman's correlation coefficient ρ between change of visual acuity and OCT parameter at each time point is shown. $^*p < 0.05$; $^{**}p < 0.01$; $^{***}p < 0.001$.

| Change of OCT parameters at the same time period | Change in visual acuity | |
	Baseline to year 3	Baseline to year 5
Pooled EZR	-0.21	-0.41*
Pooled EZR-RPE distance	0.21	0.33*
Central EZR	-0.31**	-0.44**
Central EZ-RPE distance	0.26*	0.21
CRT	0.40**	0.34*
Macular volume	0.40**	0.07

Likewise, for prediction of VA at year 2, when controlled for age at treatment initiation, injection frequency per year, and VA after 1 year, 1-year pooled ($R^2 = 0.52$, $p < 0.001$) and central EZR ($R^2 = 0.53$, $p < 0.001$) as well as 1-year pooled ($R^2 = 0.50$, $p < 0.001$) and central ($R^2 = 0.50$, $p < 0.001$) EZ-RPE distance predicted change in VA at year 2. We further evaluated the predictive value of age at treatment initiation for EZ restoration after 1 and 3 years. For this purpose, regression models were controlled for injection frequency in the first year, baseline VA, and baseline c-EZR or p-EZR. Adding age at treatment initiation as an additional independent variable, R^2 increased from 0.40 to 0.46 ($p < 0.001$) for the prediction of c-EZR at 1 year and from 0.57 to 0.62 ($p = 0.004$) for the prediction of p-EZR after 1 year. It suggests that age at treatment initiation as a single

variable explained approximately 5-6% of the variation of c-EZR and p-EZR after 1 year. However, this relationship was not significant for the prediction of 3-year EZ integrity with 1-year VA, injection frequency per year, c-EZR, and p-EZR ($p > 0.05$).

4. Discussion

We investigated the long-term changes of ellipsoid zone integrity during anti-VEGF therapy in DME patients in a real-world setting by evaluating the efficacy of EZ parameters in correlating and predicting VA outcomes at different time points. We followed patients for three years and five years after treatment initiation, in marked contrast to previous analyses which looked at functional and structural outcomes in diabetic patients over an observational period of mostly one year [7, 12, 30]. One earlier study did include clinical data of up to 4 years but did not include OCT parameters. [21] We focused on using OCT data. Previous studies included structural OCT parameters such as ellipsoid zone reflectivity, but mostly this was a qualitative analysis undertaken by masked graders, who categorized the grade of EZ disruption, or if a quantitative analysis was performed then it mostly was done manually [15, 18, 31]. Both qualitative and manual quantitative methods can be laborious and can potentially introduce bias from subjective judgment. Additionally, subtle differences in gray pixel values may be difficult to detect by masked graders. Recently, semi- or fully automated quantification methods were developed to facilitate objective analysis [32, 33]. In our study, we took advantage of image preprocessing and EZ parameters that we obtained in an automated way and included the average of 27 measurements of each fovea-centered OCT B-scan. Furthermore, we assessed both pooled and central EZ parameters to evaluate if the number and location of regions of interest affect the correlations between VA und EZ integrity. Notably, the correlation coefficient between central EZR and VA was slightly higher than pooled EZR at specific follow-up time points (years 1 and 3). The difference was considerably small. However, it hints that analyzing the central $2000\,\mu$m with multiple measurements might be sufficient for EZ analysis. Involving the entire OCT B-scan for analysis did not lead to a better correlation between VA and EZ integrity. Changes of c-EZR from baseline to year 5 were more strongly correlated to change of VA from baseline to year 5 than CRT. This was already described by Shen et al. when they retrospectively evaluated EZ, ELM, CRT, and VA outcome in 40 DME patients [34]. Overall, correlation between EZ-RPE distance and VA was lower than correlation between EZR and VA. Changes of macular edema or retinal thickening which altered the retinal anatomy might have compromised distance measurements. It is questionable if volumetric quantification as performed by Ehlers et al. in en-face OCT projections can alleviate these limitations [10, 35]. Overall, we observed similar strength of correlations between EZ parameters and VA as in enface analysis used by Ehlers' group. In addition, Ehlers et al. used research-based software for EZ mapping that is not readily available to wide-spread clinical usage. In contrast, obtaining EZ reflectance profiles as performed in this study can be easily accomplished by clinicians by using the open-source platform Fiji.

Our results were in accordance with previous studies, which demonstrated that EZR was directly correlated to VA [14] and VA improvement in the first year of treatment [10, 16, 31, 36]. De et al. analyzed the integrity of the ELM and EZ in treatment-naive DME patients at baseline and after three injections [18]. Subsequent restoration of ellipsoid zone was observed after three injections. Otani et al. retrospectively studied cross-sectional OCT B-scans in 154 eyes with DME and demonstrated that the length of preserved ELM and photoreceptor inner segment/outer segment junction (currently termed EZ) at the fovea correlated with VA [37]. Ehlers et al. conducted a posthoc analysis of the VISTA study and analyzed the EZ integrity in 106 eyes of DME patients over approximately 2 years [10]. The authors concluded that in contrast to EZ parameters, subretinal fluid volume, central subfield retinal volume, and thickness were not significantly correlated to VA after 2 years. They found out that several EZ parameters such as central EZ-RPE volume and thickness were associated with VA throughout the follow-up period.

In our study, a significant correlation between EZ integrity and VA was observed until 5 years after initiation of therapy. We found that the most contributing predictor for VA outcome was baseline VA, a finding which has been reported previously by several authors [35, 38, 39]. Combined with EZ parameters, multivariable linear regression models showed that the visual outcome at 1 year can be predicted. Our study showed that age at treatment initiation has a predictive value for the EZ restoration at 1 year, which supports previous reports about increasing age being a negative predictive factor for final VA outcome [40]. These results underline the potential utility of EZ parameters as predictive OCT biomarkers to estimate VA changes after 1 year, which has been described in several retinal diseases associated with macular edema [10, 12, 18, 19, 35]. Further studies with prospective design and larger cohorts are needed to evaluate the predictive value of these biomarkers on overall outcomes and potential improvement in disease management in patients with diabetic macular edema.

The strengths of our study include the relatively long follow-up time of up to 5 years, the real-world setup, and the automated quantification of ellipsoid zone parameters. The limitations of our real-world study included its retrospective design, small cohort size, and nonstandardized VA assessment instead of the use of ETDRS charts. The study cohort is heterogeneous due to different onset of treatment initiation, follow-up time, and individualized combination of different anti-VEGF agents as well as dexamethasone implants. These are critical aspects of a real-world study that may negatively impact the main findings. The effects of different anti-VEGF agents on EZ integrity may differ, but this was not evaluated in the current study. Larger cohort size would enable stratification of patients into subgroups according to clinical or anatomical features which could prove to be helpful in characterizing the value of EZ parameters as biomarkers for individualizing the course of treatment. For instance, Chatziralli et al. observed that the

extent of EZ restoration was dependent on the pattern of diabetic macular edema after 1 year of ranibizumab treatment in DME patients. Therefore, stratifying according to DME subtypes may enable better understanding of the retinal dynamics in treatment response. The lower injection frequency that we noted in the first year in the 5-year cohort was likely due to different treatment protocols at an earlier time. However, total injection frequency per year was nonsignificantly different in both 3-year and 5-year cohort, so that baseline characteristics are overall evenly distributed in the entire cohort. In addition, regression analysis was controlled for injection frequency.

In this study, we did not include other OCT biomarkers that might affect visual outcome in DME, such as hyperreflective foci or disorganization of the inner retinal layers (DRILs) [15, 41]. Nadri et al. found out that DRILs were correlated to the severity of diabetic retinopathy and EZ disruption [15]. Sun et al. confirmed that DRILs had predictive values for short-term VA outcome at 1 year [41]. However, including more biomarkers that are related to each other in a regression model might lead to an overfitted model, one that can be challenging to interpret and to evaluate the effect of single variables. Here, we focused on EZ changes and its direct correlation to VA changes; therefore, other OCT parameters were excluded.

All our patients received anti-VEGF agents as first line therapy; therefore, the isolated effect of dexamethasone on OCT biomarkers such as EZ integrity was not evaluated. EZ integrity has been identified as a positive predictor for VA gain in patients with treatment naive or refractory DME who received dexamethasone implants [42, 43]. Our findings support a positive correlation between EZ restoration and VA improvement. However, Zur et al. did not follow morphologic parameters after dexamethasone implantation; hence, it remains unclear how dexamethasone affects EZ restoration in eyes with treatment naive DME [42]. It is suggested that dexamethasone and anti-VEGF agents target different pathophysiological pathways [44]. The anti-inflammatory effect of dexamethasone may provide a better resolution of OCT biomarkers that presumably represent signs of retinal inflammatory response such as hyperreflective foci or serous detachment of neuroepithelium [45]. In our study, we observed a decline of EZ restoration after 3 years but did not further investigate the relationship between EZ integrity and other biomarkers. The potential association between EZ restoration and severity of retinal inflammatory signs in DME is an interesting aspect that has not been fully elucidated. Overall, further studies are needed to evaluate the long-term changes of VA and OCT biomarkers in DME treated with anti-VEGF or dexamethasone as first-line agents.

5. Conclusions

In summary, relative ellipsoid zone reflectivity ratio represents an additional potential biomarker to evaluate the course of anti-VEGF treatment in DME patients. Our results confirmed the relationship between EZ integrity and VA changes from baseline to year 5 and thus demonstrated the relationship beyond 1 year after initiation of therapy. However, further

investigation is needed to evaluate the predictive value of EZ integrity as a biomarker on the overall outcome.

Data Availability

The data used to support the findings of this study are included within the article.

Conflicts of Interest

Acknowledgments

References

[1] T. A. Ciulla, A. G. Amador, and B. Zinman, "Diabetic retinopathy and diabetic macular edema: pathophysiology, screening, and novel therapies," *Diabetes Care*, vol. 26, no. 9, pp. 2653–2664, 2003.

[2] T. Y. Wong, R. Klein, F. M. A. Islam et al., "Diabetic retinopathy in a multi-ethnic cohort in the United States," *American Journal of Ophthalmology*, vol. 141, no. 3, pp. 446–455.e1, 2006.

[3] X. W. Xie, L. Xu, Y. X. Wang, and J. B. Jonas, "Prevalence and associated factors of diabetic retinopathy. The Beijing Eye Study 2006," *Graefe's Archive for Clinical and Experimental Ophthalmology*, vol. 246, no. 11, pp. 1519–1526, 2008.

[4] P. Mitchell and T. Y. Wong, "Management Paradigms for Diabetic Macular Edema," *American Journal of Ophthalmology*, vol. 157, no. 3, pp. 505–513.e8, 2014.

[5] M. W. Stewart, "Anti-VEGF therapy for diabetic macular edema," *Current Diabetes Reports*, vol. 14, no. 8, p. 510, 2014.

[6] U. Schmidt-Erfurth, J. Garcia-Arumi, F. Bandello et al., "Guidelines for the management of diabetic macular edema by the European Society of Retina Specialists (EURETINA)," *Ophthalmologica*, vol. 237, no. 4, pp. 185–222, 2017.

[7] I. Chatziralli, D. Kazantzis, G. Theodossiadis, P. Theodossiadis, and T. Sergentanis, "Retinal layers changes in patients with diabetic macular edema treated with intravitreal anti-VEGF agents: long-term outcomes of a spectral-domain OCT study," *Ophthalmic Research*, vol. 64, no. 2, pp. 230–236, 2021.

[8] A. Markan, A. Agarwal, A. Arora, K. Bazgain, V. Rana, and V. Gupta, "Novel imaging biomarkers in diabetic retinopathy and diabetic macular edema," *Therapeutic Advances in Ophthalmology*, vol. 12, article 251584142095051, 2020.

[9] L. W. Tao, Z. Wu, R. H. Guymer, and C. D. Luu, "Ellipsoid zone on optical coherence tomography: a review," *Clinical & Experimental Ophthalmology*, vol. 44, no. 5, pp. 422–430, 2016.

[10] J. P. Ehlers, A. Uchida, M. Hu et al., "Higher-order assessment of OCT in diabetic macular edema from the VISTA study: ellipsoid zone dynamics and the retinal fluid index," *Ophthalmology Retina*, vol. 3, no. 12, pp. 1056–1066, 2019.

[11] Y. Gong, L. J. Chen, C. P. Pang, and H. Chen, "Ellipsoid zone optical intensity reduction as an early biomarker for retinitis pigmentosa," *Acta Ophthalmologica*, vol. 99, no. 2, pp. e215–e221, 2021.

[12] M. J. Tsai and C. K. Cheng, "Patterns of ellipsoid zone change associated with visual outcome for diabetic macular oedema," *Clinical & Experimental Optometry*, pp. 1–7, 2021.

[13] T. A. Ciulla, B. Kapik, D. S. Grewal, and M. S. Ip, "Visual Acuity in Retinal Vein Occlusion, Diabetic, and Uveitic Macular Edema: Central Subfield Thickness and Ellipsoid Zone Analysis," *Ophthalmology Retina*, vol. 5, no. 7, pp. 633–647, 2021.

[14] A. S. Maheshwary, S. F. Oster, R. M. S. Yuson, L. Cheng, F. Mojana, and W. R. Freeman, "The Association Between Percent Disruption of the Photoreceptor Inner Segment- Outer Segment Junction and Visual Acuity in Diabetic Macular Edema," *American Journal of Ophthalmology*, vol. 150, no. 1, pp. 63–67.e1, 2010.

[15] G. Nadri, S. Saxena, J. Stefanickova et al., "Disorganization of retinal inner layers correlates with ellipsoid zone disruption and retinal nerve fiber layer thinning in diabetic retinopathy," *Journal of Diabetes and its Complications*, vol. 33, no. 8, pp. 550–553, 2019.

[16] N. Sharef, R. Kassem, I. Hecht et al., "Interdigitation and ellipsoid zones disruption correlate with visual outcomes among treatment-naive patients with diabetic macular edema," *Ophthalmic Research*, vol. 64, no. 3, pp. 476–482, 2021.

[17] T. A. Ciulla, J. S. Pollack, and D. F. Williams, "Visual acuity outcomes and anti-VEGF therapy intensity in diabetic macular oedema: a real-world analysis of 28 658 patient eyes," *The British Journal of Ophthalmology*, vol. 105, no. 2, pp. 216–221, 2021.

[18] S. De, S. Saxena, A. Kaur et al., "Sequential restoration of external limiting membrane and ellipsoid zone after intravitreal anti-VEGF therapy in diabetic macular oedema," *Eye (London, England)*, vol. 35, no. 5, pp. 1490–1495, 2021.

[19] T. J. Gin, Z. Wu, S. K. H. Chew, R. H. Guymer, and C. D. Luu, "Quantitative analysis of the ellipsoid zone intensity in phenotypic variations of intermediate age-related macular degeneration," *Investigative Ophthalmology & Visual Science*, vol. 58, no. 4, pp. 2079–2086, 2017.

[20] I. Toprak, V. Yaylali, and C. Yildirim, "Decreased photoreceptor inner segment/outer segment junction reflectivity in patients with idiopathic epimacular membrane," *Eye (London, England)*, vol. 28, no. 9, pp. 1126–1130, 2014.

[21] E. Granstam, A. Rosenblad, A. M. Raghib et al., "Long-term follow-up of antivascular endothelial growth factor treatment for diabetic macular oedema: a four-year real-world study," *Acta Ophthalmologica*, vol. 98, no. 4, pp. 360–367, 2020.

[22] E. Van Aken, M. Favreau, E. Ramboer et al., "Real-world outcomes in patients with diabetic macular edema treated long term with ranibizumab (VISION study)," *Clinical Ophthalmology*, vol. Volume 14, pp. 4173–4185, 2020.

[23] P. Massin, C. Creuzot-Garcher, L. Kodjikian et al., "Real-world outcomes after 36-month treatment with ranibizumab 0.5 mg in patients with visual impairment due to diabetic macular edema (BOREAL-DME)," *Ophthalmic Research*, vol. 64, no. 4, pp. 577–586, 2021.

[24] B. BÄK, *Arbeitsgemeinschaft der Wissenschaftlichen Medizinischen Fachgesellschaften (AWMF)*, Nationale Versorgungs-sLeitlinie Prävention und Therapie von Netzhautkomplikationen bei Diabetes–Langfassung, Auflage, 2015.

[25] R. Federfuhrendes, "Statement of the German Ophthalmological Society, the Retina Society and the Professional Association of German Ophthalmologists: treatment of diabetic maculopathy (April 2013)," *Klinische Monatsblätter für Augenheilkunde*, vol. 230, no. 6, pp. 614–628, 2013.

[26] G. Deutsche Ophthalmologische, E. Retinologische Gesellschaft, and E. Berufsverband der Augenarzte Deutschlands, "Statement of the German Ophthalmological Society, the Retinological Society and the Professional Association of Ophthalmologists in Germany on treatment of diabetic macular edema: Situation August 2019," *Der Ophthalmologe*, vol. 117, no. 3, pp. 218–247, 2020.

[27] J. Schindelin, I. Arganda-Carreras, E. Frise et al., "Fiji: an open-source platform for biological-image analysis," *Nature Methods*, vol. 9, no. 7, pp. 676–682, 2012.

[28] Y. Itoh, D. Petkovsek, P. K. Kaiser, R. P. Singh, and J. P. Ehlers, "Optical coherence tomography features in diabetic macular edema and the impact on anti-VEGF response," *Ophthalmic Surgery, Lasers & Imaging Retina*, vol. 47, no. 10, pp. 908–913, 2016.

[29] O. Ugwuegbu, A. Uchida, R. P. Singh et al., "Quantitative assessment of outer retinal layers and ellipsoid zone mapping in hydroxychloroquine retinopathy," *The British Journal of Ophthalmology*, vol. 103, no. 1, pp. 3–7, 2019.

[30] T. Granström, H. Forsman, A. L. Olinder et al., "Patient-reported outcomes and visual acuity after 12 months of anti-VEGF- treatment for sight-threatening diabetic macular edema in a real world setting," *Diabetes Research and Clinical Practice*, vol. 121, pp. 157–165, 2016.

[31] S. Serizawa, K. Ohkoshi, Y. Minowa, and K. Soejima, "Interdigitation zone band restoration after treatment of diabetic macular edema," *Current Eye Research*, vol. 41, no. 9, pp. 1229–1234, 2016.

[32] S. Thiele, B. Isselmann, M. Pfau et al., "Validation of an automated quantification of relative ellipsoid zone reflectivity on spectral domain-optical coherence tomography images," *Translational Vision Science & Technology*, vol. 9, no. 11, p. 17, 2020.

[33] T. Etheridge, E. T. A. Dobson, M. Wiedenmann et al., "A semi-automated machine-learning based workflow for ellipsoid zone analysis in eyes with macular edema: SCORE2 pilot study," *PLoS One*, vol. 15, no. 4, article e0232494, 2020.

[34] Y. Shen, K. Liu, and X. Xu, "Correlation between visual function and photoreceptor integrity in diabetic macular edema: spectral-domain optical coherence tomography," *Current Eye Research*, vol. 41, no. 3, pp. 391–399, 2016.

[35] J. R. Abraham, J. Boss, A. S. Babiuch et al., "Longitudinal assessment of ellipsoid zone mapping parameters in retinal venous occlusive disease with associated macular edema," *Journal of VitreoRetinal Diseases*, vol. 5, no. 1, pp. 40–45, 2021.

[36] I. Chatziralli, G. Theodossiadis, E. Dimitriou, D. Kazantzis, and P. Theodossiadis, "Association between the patterns of diabetic macular edema and photoreceptors' response after intravitreal ranibizumab treatment: a spectral-domain optical coherence tomography study," *International Ophthalmology*, vol. 40, no. 10, pp. 2441–2448, 2020.

[37] T. Otani, Y. Yamaguchi, and S. Kishi, "Correlation between visual acuity and foveal microstructural changes in diabetic macular edema," *Retina*, vol. 30, no. 5, pp. 774–780, 2010.

[38] J. Choovuthayakorn, A. Tantraworasin, P. Phinyo et al., "Factors associated with 1-year visual response following intravitreal bevacizumab treatment for diabetic macular edema: a retrospective single center study," *Int J Retina Vitreous*, vol. 7, no. 1, p. 17, 2021.

[39] J. Choovuthayakorn, P. Phinyo, A. Tantraworasin et al., "Intravitreal anti-vascular endothelial growth factor therapy for diabetic macular edema in clinical practice of single center: three-year outcomes," *Ophthalmic Research*, vol. 64, no. 3, pp. 483–493, 2021.

[40] I. Chatziralli, P. Theodossiadis, E. Parikakis et al., "Dexamethasone intravitreal implant in diabetic macular edema: real-life data from a prospective study and predictive factors for visual outcome," *Diabetes Therapy*, vol. 8, no. 6, pp. 1393–1404, 2017.

[41] J. K. Sun, S. H. Radwan, A. Z. Soliman et al., "Neural retinal disorganization as a robust marker of visual acuity in current and resolved diabetic macular edema," *Diabetes*, vol. 64, no. 7, pp. 2560–2570, 2015.

[42] D. Zur, M. Iglicki, C. Busch et al., "OCT biomarkers as functional outcome predictors in diabetic macular edema treated with dexamethasone implant," *Ophthalmology*, vol. 125, no. 2, pp. 267–275, 2018.

[43] A. Meduri, G. W. Oliverio, L. Trombetta, M. Giordano, L. Inferrera, and C. J. Trombetta, "Optical Coherence Tomography Predictors of Favorable Functional Response in Naïve Diabetic Macular Edema Eyes Treated with Dexamethasone Implants as a First-Line Agent," *Journal of Ophthalmology*, vol. 2021, Article ID 6639418, 5 pages, 2021.

[44] P. Romero-Aroca, "Targeting the pathophysiology of diabetic macular edema," *Diabetes Care*, vol. 33, no. 11, pp. 2484-2485, 2010.

[45] I. Ceravolo, G. W. Oliverio, A. Alibrandi et al., "The application of structural retinal biomarkers to evaluate the effect of intravitreal ranibizumab and dexamethasone intravitreal implant on treatment of diabetic macular edema," *Diagnostics (Basel)*, vol. 10, no. 6, p. 413, 2020.

Research Article

Correlation between Imaging Morphological Findings and Laboratory Biomarkers in Patients with Diabetic Macular Edema

Eleni Dimitriou,[1] Theodoros N. Sergentanis,[2] Vaia Lambadiari,[3] George Theodossiadis,[1] Panagiotis Theodossiadis,[1] and Irini Chatziralli [1]

[1]*2nd Department of Ophthalmology, National and Kapodistrian University of Athens, Athens, Greece*
[2]*Department of Clinical Therapeutics, Alexandra Hospital, Medical School, National and Kapodistrian University of Athens, Athens, Greece*
[3]*2nd Department of Internal Medicine, Research Institute and Diabetes Center, National and Kapodistrian University of Athens, Athens, Greece*

Correspondence should be addressed to Irini Chatziralli; eirchat@yahoo.gr

Eleni Dimitriou and Theodoros N. Sergentanis contributed equally to this work.

Purpose. To investigate the potential association between peripheral blood biomarkers and morphological characteristics of retinal imaging in patients with diabetic macular edema (DME). *Methods.* Participants in this cross-sectional study were 36 consecutive patients (36 eyes) with treatment-naïve DME, who underwent spectral domain-optical coherence tomography (SD-OCT), fundus photography, and fundus fluorescein angiography (FFA). In addition, peripheral blood samples were taken to evaluate full blood count and biochemical parameters. Correlation between imaging characteristics and laboratory parameters was examined. *Results.* Eyes with central subfield thickness greater than $405\,\mu$m presented significantly higher neutrophils/lymphocytes ($p = 0.043$) and higher lipoprotein (a) compared to eyes with $CST < 405\,\mu$m ($p = 0.003$). Presence of hyperreflective foci on SD-OCT was associated with significantly higher white blood cell count ($p = 0.028$). Ellipsoid zone disruption was associated with significantly lower hematocrit ($p = 0.012$), hemoglobin ($p = 0.009$), and red blood cell count ($p = 0.026$), as well as with higher lipoprotein (a) ($p = 0.015$). Macular ischemia on FFA was associated with significantly higher monocytes ($p = 0.027$) and monocytes/HDL ($p = 0.019$). No significant associations were found between laboratory parameters and subretinal fluid, intraretinal fluid, exudates, cysts, disorganization of inner retinal layers, epiretinal membrane, and external limiting membrane condition. *Conclusion.* Specific imaging morphological characteristics were found to be associated with laboratory parameters in patients with DME. These findings may shed light on the pathophysiology of DME and its correlation with the development of specific clinical signs.

1. Introduction

Diabetic macular edema (DME) is the most common cause of visual impairment in patients with diabetes mellitus (DM), characterized by exudation and accumulation of extracellular fluid in the macula [1, 2]. The overall prevalence of DME in patients with DM has been estimated to be about 7-14%, while it varies from 0% to 3% in patients with recent DM diagnosis and increases to 28% in patients with DM for more than 20 years [1–5].

In the pathogenesis of DME, chronic hyperglycemia promotes a cascade of biochemical pathways and consequent structural alterations in the retinal blood vessels' wall, including the loss of pericytes and the breakdown of the blood-retinal-barrier, leading to retinal vascular permeability [6, 7]. This breakdown is mainly driven by the production of inflammatory cytokines, with vascular endothelial growth factor (VEGF) to be the most prominent [6, 7]. Moreover, it has been shown that patients with DME have increased levels of proinflammatory mediators in aqueous humor com-

pared to non-DME cases [8], while there is a controversy whether the pathophysiology of DME is mainly attributed to such systemic affection or to a local intraocular response. Of note, several studies have shown that elevated serum lipids, including cholesterol and low-density lipoprotein (LDL), demonstrated a significant association with retinal hard exudates and formation of DME [9–12], while elevated IL-6 has also been correlated with diffuse retinal thickness or severity of DME [13, 14].

Nowadays, there is a great development in retinal imaging, especially with the advent of spectral domain-optical coherence tomography (SD-OCT) and swept source-OCT (SS-OCT) [15, 16], as well as OCT angiography [17, 18]. Both OCT and OCTA are noninvasive techniques, enabling the identification of specific morphological characteristics of DME, while OCTA allows the quantification of the foveal avascular zone (FAZ) area besides vessel density [18].

Given the current understanding of DME pathogenesis, although much reported information exists on intraocular biomarkers in patients with DME, literature is scarce regarding systemic biomarkers and their correlation with morphological characteristics in retinal imaging. Ghosh et al. examined the relationship between different OCT patterns of DME and systemic risk factors in patients with DME and did not identify any modifiable systemic factor for any of the OCT patterns in DME [19].

Based on the above, the purpose of the present study was to investigate the potential association between peripheral blood biomarkers and morphological characteristics of retinal imaging in patients with DME.

2. Methods

Participants in this observational, cross-sectional study were 36 consecutive patients with DM type 2 and treatment naïve DME, who were diagnosed and treated at the 2nd Department of Ophthalmology, National and Kapodistrian University of Athens, Athens, Greece, between 1st September 2019 and 31st March 2020. The study protocol adhered to the tenets of the Declaration of Helsinki and was approved by the Institutional Review Board. Written informed consent was obtained from all participants.

All patients had nonproliferative diabetic retinopathy (NPDR) and treatment naïve DME, confirmed on SD-OCT, revealing central subfield thickness (CST) $\geq 320\,\mu$m. One eye of each patient was included. In cases of bilateral DME, the right eye was chosen, so as to avoid selection bias. Patients with other vitreoretinal diseases, uveitis, media opacities, previous vitreoretinal surgery, previous laser photocoagulation, or ocular surgery in the previous 6 months were excluded.

Demographic data of patients (age, gender) were recorded, along with the duration of DM. All participants underwent a complete ophthalmologic examination, including best-corrected visual acuity (BCVA) measurement by means of Snellen's charts (converted to logMAR scale), slit-lamp examination, dilated fundoscopy, color fundus photography using Topcon TRC-50DX (Topcon Corporation), SD-OCT, and fundus fluorescein angiography (FFA) using Spectralis (Spectralis HRA+OCT, Heidelberg Engi-

neering, Heidelberg, Germany). SD-OCT was obtained using a standard acquisition protocol; six radial scans 3 mm long were performed at equally spaced angular orientations centered on the foveola. The OCT volume scan was performed on a 20×20 degree cube, consisted of 49 horizontal B-scans with 20 averaged frames per B-scan centered over the fovea. The following SD-OCT variables were recorded at baseline: CST (μm), presence of intraretinal fluid (IRF), sub-retinal fluid (SRF), cysts, hyperreflective foci (HF), and disorganization of the inner retinal layers (DRIL) and epiretinal membrane (ERM). Ellipsoid zone (EZ) and external limiting membrane (ELM) condition were also assessed. In addition, the presence of exudates on color fundus photography was recorded. The severity of DR was based on color fundus photography and on FFA and was graded according to the international diabetic retinopathy disease severity scale [20]. Moreover, macular ischemia was evaluated on FFA and defined as disruption and enlargement of foveal avascular zone (FAZ). Two investigators (IC, ED) independently evaluated qualitatively the SD-OCT images, the fundus photographs, and the FFA images. The interobserver agreement ranged from very good to perfect for all SD-OCT parameters ($k = 0.999$ for IRF; $k = 0.999$ for SRF; $k = 0.872$ for HF; $k = 0.851$ for DRIL; $k = 0.999$ for ERM; $k = 0.902$ for EZ condition; and $k = 0.883$ for ELM condition), as well as for DR severity assessment on fundus photographs ($k = 0.901$) and ischemia evaluation on FFA ($k = 0.935$).

At the same day and following an eight hour overnight fast, all patients underwent a forearm venous puncture for peripheral blood extraction and serum was separated. Full blood count was measured on a Sysmex XE-2100 analyzer (Sysmex Corp. Kobe, Japan), while all biochemical analyses were performed on a Roche Cobas 8000 (Roche, Chicago, IL, USA) in the laboratory of Attikon University Hospital. Specifically, we analyzed the following parameters: glucose, glycated Hb (HbA1c), urea, creatinine, cholesterol, HDL, LDL, triglycerides, apolipoprotein A, apolipoprotein B, lipoprotein (a), homocysteine, vitamin D, and IL-6.

2.1. Statistical Analysis. For the description of patients' characteristics, descriptive statistics were calculated; mean ± standard deviation (SD) was used for continuous variables, while relative frequencies and percentages for categorical variables were reported. All variables were tested for normal distribution with the Shapiro–Wilk test. The associations between laboratory and imaging variables were evaluated with the Mann–Whitney–Wilcoxon test (MWW), as appropriate. In addition, Pearson's chi-squared test (P) or Fisher's exact test (F) were also appropriately implemented. According to the *a priori* power calculation, a sample size of 36 eyes was adequate to achieve 80% power for the detection of an effect size larger or equal to 1.05 (in simple terms, a difference of $1.05 * SD$ between the compared subgroups), assuming an application of the two-tailed Mann–Whitney–Wilcoxon test for equally sized subgroups at the 5% level of significance. The sample size calculation was performed with G * Power 3.1.9.2 software (University of Dusseldorf, Germany). Statistical analysis was performed using STATA/SE 13 statistical software (Stata Corporation, College

TABLE 1: Demographic and clinical characteristics of the study sample ($n = 36$ patients with diabetic macular edema).

Age (mean ± SD, years)	64.2 ± 8.5
Gender (n, %)	
Male	21 (58.3%)
Female	15 (41.7%)
Duration of diabetes mellitus (mean ± SD, years)	11.7 ± 4.7
HbA1c (mean ± SD, %)	8.4 ± 1.9
Stage of diabetic retinopathy (n, %)	
Mild	10 (27.8%)
Moderate	17 (47.2%)
Severe	9 (25.0%)
Best-corrected visual acuity (mean ± SD, logMAR)	0.51 ± 0.29
Imaging characteristics	
Central subfield thickness (mean ± SD, μm)	439.2 ± 79.1
Intraretinal fluid (n, %)	36 (100%)
Subretinal fluid (n, %)	9 (25%)
Cysts (n, %)	2 (5.6%)
Hyperreflective foci (n, %)	15 (41.7%)
Exudates (n, %)	13 (36.1%)
Disorganization of inner retinal layer (n, %)	6 (16.7%)
Epiretinal membrane (n, %)	2 (5.6%)
Ellipsoid zone condition (n, %)	
Intact	23 (63.9%)
Disrupted	13 (36.1%)
External limiting membrane condition (n, %)	
Intact	26 (72.2%)
Disrupted	10 (27.8%)
Macular ischemia (n, %)	9 (25%)

Station, TX, USA). A p value < 0.05 was considered statistically significant.

3. Results

The demographic and clinical characteristics of the study sample are shown in Table 1. The mean age of patients was 64.2 ± 8.5 years. 58.3% of patients were male and 41.7% female. The mean duration of DM was 11.7 ± 4.7 years. The mean BCVA was 0.51 ± 0.29 logMAR, while the mean CST was 439.2 ± 79.1 μm.

Regarding the potential association between imaging characteristics and laboratory variables, no significant correlations were found for IRF, SRF, exudates, cysts, DRIL, ERM, and ELM condition.

Table 2 shows the comparison of laboratory parameters between eyes with HF ($n = 15$) and without HF ($n = 21$). Eyes with HF presented significantly higher white blood cell (WBC) count compared to those without HF ($p = 0.028$, MWW).

Table 3 shows the comparison of laboratory parameters between eyes with intact EZ ($n = 23$) and those with disrupted EZ ($n = 13$). Eyes with disrupted EZ presented significantly lower hematocrit ($p = 0.012$, MWW) and hemoglobin

TABLE 2: Association between laboratory variables and hyperreflective foci on optical coherence tomography. Laboratory variables are summarized as median (IQR: interquartile range).

	HF present ($n = 15$)	HF absent ($n = 21$)	p value (MWW)
Red blood cells ($10^6/\mu$l)	4.65 (0.61)	4.73 (0.91)	0.824
White blood cells ($10^3/\mu$l)	8.54 (2.10)	7.29 (2.26)	**0.028**
Neutrophils ($10^3/\mu$l)	5.24 (2.08)	4.37 (1.41)	0.124
Lymphocytes ($10^3/\mu$l)	2.30 (1.01)	1.91 (0.61)	0.096
Monocytes ($10^3/\mu$l)	0.63 (0.20)	0.51 (0.27)	0.260
Platelets ($10^3/\mu$l)	248 (37)	219 (78)	0.073
Hematocrit (%)	40.6 (4.1)	40.7 (3.5)	0.547
Hemoglobin (g/dl)	13.9 (1.5)	13.4 (1.5)	0.419
Monocytes/lymphocytes	0.27 (0.14)	0.29 (0.19)	0.962
Neutrophils/lymphocytes	2.15 (0.92)	2.25 (1.36)	0.937
Monocytes/HDL	0.013 (0.006)	0.011 (0.007)	0.516
Glucose (mg/dl)	198 (87)	161 (81)	0.084
HbA1c (%)	8.8 (2.5)	7.8 (1.8)	0.281
Urea (mg/dl)	37.8 (10.8)	37.5 (23.6)	0.635
Creatinine (mg/dl)	0.8 (0.2)	0.9 (0.7)	0.168
Cholesterol (mg/dl)	172 (61)	147 (56)	0.384
LDL (mg/dl)	94 (56)	80 (44)	0.310
HDL (mg/dl)	45 (14)	47 (17)	0.975
Triglycerides (mg/dl)	170 (168)	122 (89)	0.059
IL-6 (pg/ml)	3.5 (3.7)	3.8 (2.2)	0.680
Apolipoprotein A (mg/dl)	145 (35)	141 (37)	0.334
Apolipoprotein B (mg/dl)	89 (44)	77 (34)	0.228
Lipoprotein (a) (nmol/l)	28.7 (38.6)	15.4 (107.3)	0.975
Homocysteine (μmol/l)	14.7 (7.4)	17.8 (11.2)	0.141
Vitamin D (ng/ml)	19.8 (12.7)	21.6 (18.1)	0.506

HF: hyperreflective foci; MWW: Mann–Whitney–Wilcoxon's test.

(Hb) ($p = 0.009$, MWW), as well as lower red blood cell (RBC) count ($p = 0.026$, MWW), while they had significantly higher lipoprotein (a) compared to eyes with intact EZ ($p = 0.015$, MWW).

Table 4 shows the comparison of laboratory parameters between eyes with macular ischemia ($n = 9$) and those without macular ischemia ($n = 27$). Eyes with macular ischemia had significantly higher monocytes ($p = 0.027$, MWW) and monocytes/HDL ($p = 0.019$, MWW) compared to eyes without macular ischemia.

Table 5 shows the comparison of laboratory parameters between eyes with CST above or equal to median (405 μm) and those with CST below median. Eyes with CST ≥ 405 μm presented higher neutrophils/lymphocytes ($p = 0.043$, MWW) and higher lipoprotein (a) compared to eyes with CST < 405 μm ($p = 0.003$, MWW).

Figures 1 and 2 show correlation between laboratory and morphological findings in patients with DME.

TABLE 3: Association between laboratory variables and ellipsoid zone condition on optical coherence tomography. Laboratory variables are summarized as median (IQR: interquartile range).

	EZ intact ($n = 23$)	EZ disrupted ($n = 13$)	p value (MWW)
Red blood cells ($10^6/\mu l$)	4.75 (0.71)	4.38 (0.53)	**0.026**
White blood cells ($10^3/\mu l$)	7.81 (3.01)	8.09 (2.28)	0.417
Neutrophils ($10^3/\mu l$)	4.64 (2.03)	5.29 (3.02)	0.174
Lymphocytes ($10^3/\mu l$)	2.04 (0.62)	2.18 (1.00)	0.846
Monocytes ($10^3/\mu l$)	0.54 (0.22)	0.57 (0.33)	0.818
Platelets ($10^3/\mu l$)	246 (71)	241 (31)	0.737
Hematocrit (%)	41.2 (4.4)	38.7 (3.7)	**0.012**
Hemoglobin (g/dl)	14.0 (1.2)	12.9 (1.3)	**0.009**
Monocytes/lymphocytes	0.27 (0.14)	0.28 (0.22)	0.659
Neutrophils/lymphocytes	2.25 (1.25)	2.44 (1.53)	0.548
Monocytes/HDL	0.013 (0.006)	0.013 (0.007)	>0.999
Glucose (mg/dl)	177 (87)	113 (105)	0.133
HbA1c (%)	7.6 (2.3)	9.0 (1.5)	0.331
Urea (mg/dl)	36.2 (17.4)	42.3 (18.3)	0.274
Creatinine (mg/dl)	0.8 (0.2)	1.0 (0.7)	0.143
Cholesterol (mg/dl)	153 (64)	166 (39)	0.584
LDL (mg/dl)	86 (55)	87 (43)	0.902
HDL (mg/dl)	45 (19)	50 (11)	0.584
Triglycerides (mg/dl)	131 (149)	138 (120)	0.596
IL-6 (pg/ml)	3.4 (2.1)	4.5 (8.0)	0.377
Apolipoprotein A (mg/dl)	142 (36)	143 (13)	0.750
Apolipoprotein B (mg/dl)	82 (42)	84 (25)	0.724
Lipoprotein (a) (nmol/l)	14.7 (34.8)	89.5 (188.4)	**0.015**
Homocysteine ($\mu mol/l$)	15.2 (8.0)	18.9 (8.7)	0.197
Vitamin D (ng/ml)	23 (18.1)	25.4 (9.8)	0.090

EZ: ellipsoid zone; MWW: Mann–Whitney–Wilcoxon's test.

TABLE 4: Association between laboratory variables and macular ischemia on fluorescein angiography. Laboratory variables are summarized as median (IQR: interquartile range).

	Macular ischemia presence ($n = 9$)	Macular ischemia absence ($n = 27$)	p (MWW)
Red blood cells ($10^6/\mu l$)	4.65 (0.73)	4.70 (0.82)	0.932
White blood cells ($10^3/\mu l$)	9.0 (2.49)	7.57 (1.96)	0.096
Neutrophils ($10^3/\mu l$)	5.24 (1.96)	4.57 (2.03)	0.074
Lymphocytes ($10^3/\mu l$)	2.33 (1.87)	2.03 (0.46)	0.718
Monocytes ($10^3/\mu l$)	0.64 (0.38)	0.51 (0.19)	**0.027**
Platelets ($10^3/\mu l$)	243 (86)	244 (72)	0.430
Hematocrit (%)	40.5 (6.4)	40.7 (5.3)	0.503
Hemoglobin (g/dl)	13.2 (1.4)	13.9 (1.4)	0.345
Monocytes/lymphocytes	0.29 (0.21)	0.27 (0.14)	0.159
Neutrophils/lymphocytes	2.15 (2.95)	2.25 (0.99)	0.718
Monocytes/HDL	0.016 (0.010)	0.011 (0.004)	**0.019**
Glucose (mg/dl)	198 (219)	167 (62)	0.606
HbA1c (%)	9.4 (3.0)	7.4 (1.8)	0.074
Urea (mg/dl)	40 (16.8)	35.8 (20)	0.154
Creatinine (mg/dl)	0.8 (0.5)	0.8 (0.2)	0.889
Cholesterol (mg/dl)	172 (80)	147 (55)	0.216
LDL (mg/dl)	98 (68)	80 (43)	0.287
HDL (mg/dl)	43 (16)	48 (19)	0.390
Triglycerides (mg/dl)	211 (190)	128 (70)	0.198
IL-6 (pg/ml)	4.2 (6.2)	3.0 (2.5)	0.149
Apolipoprotein A (mg/dl)	141 (33)	143 (34)	0.606
Apolipoprotein B (mg/dl)	93 (63)	81 (33)	0.363
Lipoprotein (a) (nmol/l)	34.7 (92.6)	15.4 (59.6)	0.363
Homocysteine ($\mu mol/l$)	17.8 (6.8)	15.7 (8)	0.731
Vitamin D (ng/ml)	17.9 (13)	21.6 (12.3)	0.668

MWW: Mann–Whitney–Wilcoxon's test.

4. Discussion

The principal message of the study is that most of the imaging morphological characteristics studied herein were not correlated with laboratory parameters in patients with DME, suggesting that DME may be mainly attributed to a local response more than a systemic effect. However, CST and specific OCT biomarkers, i.e., HF and EZ conditions, as well as macular ischemia on FFA, were found to be associated with laboratory findings in patients with DME, shedding light on the pathophysiology of DME and its correlation with the development of these specific clinical characteristics.

Firstly, lipoprotein (a) was found to be associated with high CST and with EZ disruption. Previous studies have shown that high lipoprotein (a) concentration was independently associated with the presence and severity of DR in patients with type 2 DM, regardless of glycemic control [21–25]. Specifically, lipoprotein (a) can affect vascular tone

and perfusion, oxidize lipids, and enhance oxidative stress via the generation of reactive oxygen species and inflammatory actions on the vascular wall [26, 27]. Moreover, lipoprotein (a) has been associated with endothelial dysfunction, suggesting that it could be an independent risk factor for diabetic microvascular complications [28, 29]. Although the exact mechanism behind the potential causal relationship between lipoprotein (a) and DME, and especially EZ disruption, remains unclear, it has been hypothesized that elevated lipoprotein (a) concentrations may play a causative role in DME by damaging the microcirculation [30]. In addition, lipoprotein (a) has been involved in the activation of acute inflammation and may be related to more severe DR, including DME severity with higher CST and EZ disruption [31]. Ellipsoid zone disruption has also been associated with decreased RBC count, decreased Hb, and consequently, decreased hematocrit. In patients with DM, RBC have been

TABLE 5: Association between laboratory variables and central subfield thickness on optical coherence tomography. Laboratory variables are summarized as median (IQR: interquartile range).

	Central subfield thickness $\geq 405\,\mu$m ($n = 18$)	Central subfield thickness $< 405\,\mu$m ($n = 18$)	p (MWW)
Red blood cells ($10^6/\mu$l)	4.6 (0.48)	4.79 (0.76)	0.097
White blood cells ($10^3/\mu$l)	7.7 (3.31)	7.87 (1.95)	0.728
Neutrophils ($10^3/\mu$l)	5.0 (3.0)	4.64 (1.74)	0.174
Lymphocytes ($10^3/\mu$l)	1.97 (0.76)	2.08 (1.02)	0.282
Monocytes ($10^3/\mu$l)	0.57 (0.29)	0.54 (0.20)	0.824
Platelets ($10^3/\mu$l)	241 (82)	251 (68)	0.359
Hematocrit (%)	40.5 (4.7)	40.9 (4.1)	0.728
Hemoglobin (g/dl)	13.3 (1.5)	13.9 (1.0)	0.516
Monocytes/lymphocytes	0.28 (0.20)	0.27 (0.17)	0.268
Neutrophils/lymphocytes	2.74 (1.34)	1.95 (0.72)	**0.043**
Monocytes/HDL	0.012 (0.007)	0.013 (0.006)	0.950
Glucose (mg/dl)	159 (92)	180 (97)	0.179
HbA1c (%)	8.2 (2.3)	7.6 (3.4)	0.924
Urea (mg/dl)	37 (19)	38.9 (17.1)	0.812
Creatinine (mg/dl)	0.9 (0.5)	0.8 (0.2)	0.608
Cholesterol (mg/dl)	163 (47)	153 (64)	0.658
LDL (mg/dl)	95 (43)	84 (55)	0.716
HDL (mg/dl)	48 (12)	45 (20)	0.924
Triglycerides (mg/dl)	137 (90)	122 (207)	0.693
IL-6 (pg/ml)	3.4 (3.6)	3.8 (1.9)	0.764
Apolipoprotein A (mg/dl)	142 (32)	144 (43)	0.937
Apolipoprotein B (mg/dl)	88 (25)	75 (56)	0.359
Lipoprotein (a) (nmol/l)	60.0 (162.1)	10.1 (17.4)	**0.003**
Homocysteine (μmol/l)	18.3 (10.9)	15.2 (6.9)	0.624
Vitamin D (ng/ml)	21.7 (13.0)	21.3 (18.7)	0.776

MWW: Mann–Whitney–Wilcoxon's test.

shown to present variations in size and diameter [32]. Chronic hyperglycemia can lead to nonenzymatic glycation of RBC membrane proteins that would accelerate RBC aging due to negative surface electrical charge [32, 33]. The RBC count has been found to be reduced in patients with microvascular complications, especially in those with longer DM duration [32–34]. Since Hb levels are directly correlated with RBC count, reduced RBC would reflect on Hb concentration and on hematocrit. In our case with DME, hyperglycemia induces the rearrangement of proteins in the plasma membrane, while cytoskeleton proteins also appear to be heavily glycosylated, affecting membrane stability, as it has been mentioned in RBC membrane proteins [32]. Therefore, reduced RBC could represent more severe DR and DME, which may be reflected on EZ disruption, as a result of cytoskeleton weakening.

An interesting finding of our study was the association between HF and WBC. Many theories have attempted to explain the pathophysiology of HF, but their precise nature remains elusive. Framme et al. suggested that HF can be leucocytes or RPE cells, indicating retinal inflammation [35]. Coscas et al. supported this concept and postulated that HF

are microglia cells activated by inflammation [36]. White blood cells and their subtypes are the biomarkers of inflammatory response because their activation leads to the synthesis of inflammatory cytokines, as it has been previously identified in patients with DR [37, 38]. Therefore, our finding that HF presence was associated with increased WBC is consistent with the hypothesis that an inflammatory component is implemented in HF pathogenesis [39–41].

In recent studies, neutrophil (an indicator of inflammation) to lymphocyte (an indicator of physiologic stress) ratio was evaluated in inflammatory diseases, such as coronary artery disease, noncardiac diseases, retinal vein occlusion, age-related macular degeneration and DR [42–47]. Of note, neutrophil-to-lymphocyte ratio is more powerful for prediction of inflammatory diseases than subtypes of WBC alone because it combines the predictive values of two parameters of WBC [44]. In DME, the chronic low-grade inflammation may lead to inflammatory cytokine release, which is commonly responsible for increased vascular permeability [7]. As a result, neutrophil-to-lymphocyte ratio may be defined as an indication of subclinical inflammation, especially in more severe DME, as it was found in our study, showing a
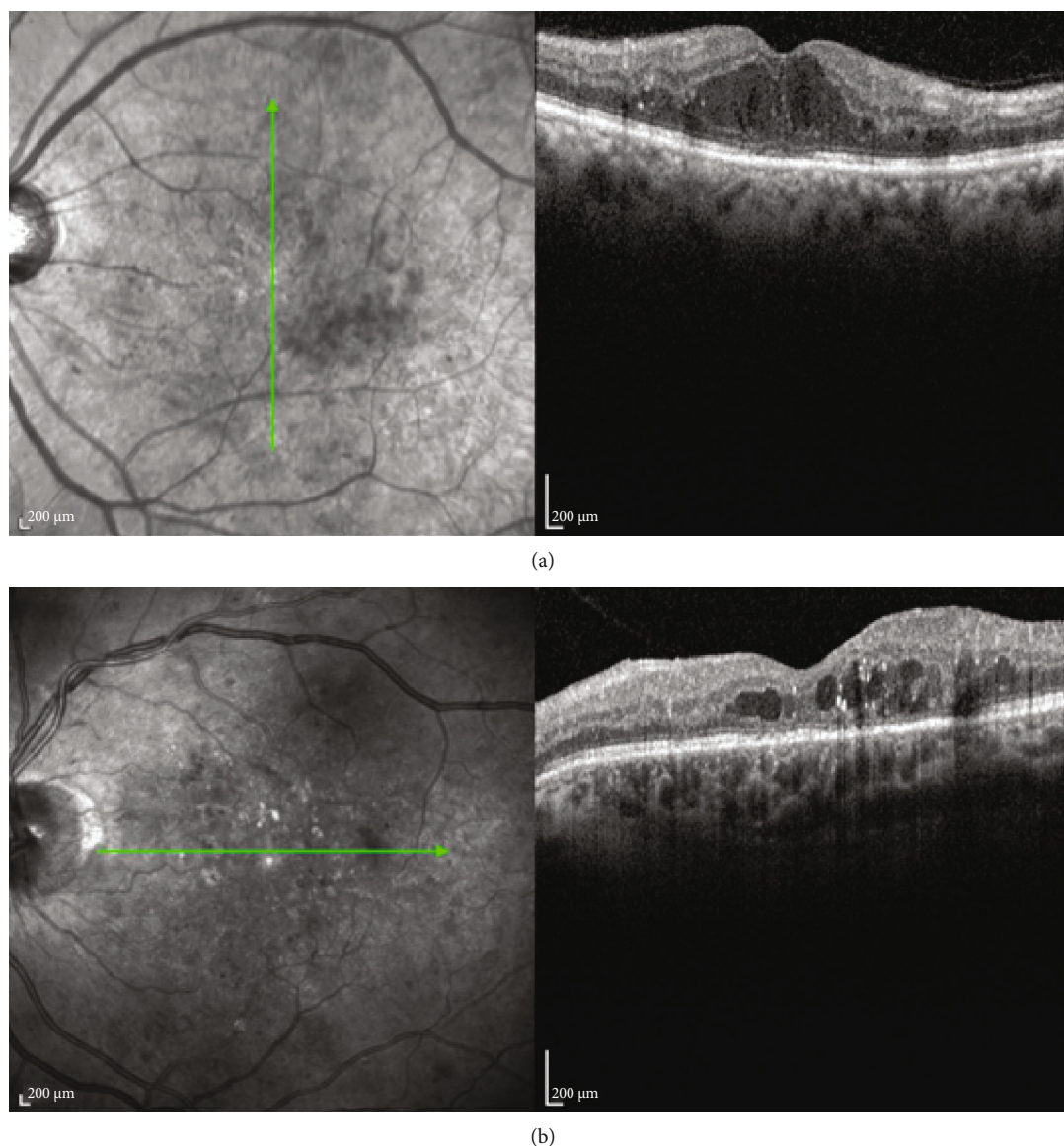
(a)

(b)

FIGURE 1: (A) Optical coherence tomography of a female patient with diabetic macular edema and elevated lipoprotein (a), as well as decreased hematocrit and red blood count, which was associated with the disruption of the ellipsoid zone and an increase in central subfield thickness. (B) Optical coherence tomography of a male patient with diabetic macular edema and elevated white blood cells, which were associated with the presence of hyperreflective foci.

significant association between increased neutrophil-to-lymphocyte ratio and higher CST.

Moreover, monocyte-to-HDL ratio has been investigated as a new inflammation biomarker and is considered superior to subtypes of WBC, especially in patients with cardiovascular and cerebrovascular diseases, as well as in patients with branch retinal vein occlusion [48–50]. Monocytes are indicators of inflammation, since they are responsible for inflammatory cytokine secretion, while HDL has antioxidant and anti-inflammatory effects [51, 52]. In our study, patients with macular ischemia were found to have increased monocytes, as well as monocyte-to-HDL ratio, which is consistent with other studies in patients with myocardial infarction and limb

ischemia, suggesting monocyte-to-HDL ratio as a biomarker of ischemic conditions [53, 54].

A potential limitation of this study pertains to the relatively small sample size, although our *a priori* statistical power calculation showed that it was adequate to achieve 80% power for the detection of an effect size larger or equal to 1.05; further larger studies seem necessary to validate our results.

In conclusion, this study investigated the potential correlation between imaging morphological findings and laboratory biomarkers in patients with DME. Our results showed that specific inflammatory biomarkers, such as WBC, monocytes, monocyte-to-HDL, and neutrophil-to-lymphocyte
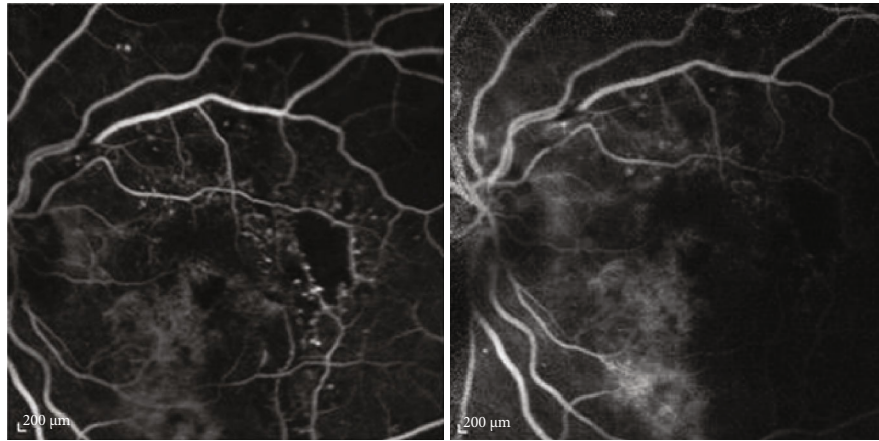
FIGURE 2: Fluorescein angiography of a male patient with diabetic macular edema, showing macular ischemia, which was associated with higher monocytes and higher monocytes/HDL.

ratios, were associated with more severe disease activity with higher CST and presence of HF and macular ischemia, while EZ disruption was found to be associated with increased lipoprotein (a) and decreased RBC, both of which were involved in microcirculation alterations in patients with DME. These findings may scrutinize the pathophysiology of DME and the pathogenesis of specific clinical signs. However, it should be noted that most of imaging biomarkers studied herein were not correlated with laboratory parameters in patients with DME, suggesting that DME may be mainly attributed to a local response more than a systemic effect. Further studies with a large sample size are needed to justify our results.

Data Availability

Data are available upon request from authors.

Conflicts of Interest

The authors declare that they have no conflicts of interest.

Authors' Contributions

Eleni Dimitriou collected and interpreted data. Theodoros Sergentanis performed the statistical analysis and interpretation of data. Vaia Lambadiari, George Theodossiadis, and Panagiotis Theodossiadis collected data, interpreted data, and critically revised the manuscript. Irini Chatziralli conceived and designed the study; collected, analyzed, and interpreted data; drafted the manuscript; and supervised the study. Eleni Dimitriou and Theodoros Sergentanis have equal contribution.

References

[1] R. Klein, B. E. Klein, S. E. Moss, M. D. Davis, and D. L. DeMets, "The Wisconsin Epidemiologic Study of Diabetic Retinopathy: IV. Diabetic Macular Edema," *Ophthalmology*, vol. 91, no. 12, pp. 1464–1474, 1984.

[2] R. Klein, B. E. Klein, and S. E. Moss, "Visual impairment in diabetes," *Ophthalmology*, vol. 91, no. 1, pp. 1–9, 1984.

[3] J. W. Yau, S. L. Rogers, R. Kawasaki et al., "Global prevalence and major risk factors of diabetic retinopathy," *Diabetes Care*, vol. 35, no. 3, pp. 556–564, 2012.

[4] R. Klein, B. E. Klein, S. E. Moss, and K. J. Cruickshanks, "The Wisconsin Epidemiologic Study of Diabetic Retinopathy XV: The Long-term Incidence of Macular Edema," *Ophthalmology*, vol. 102, no. 1, pp. 7–16, 1995.

[5] X. Zhang, J. B. Saaddine, C. F. Chou et al., "Prevalence of diabetic retinopathy in the United States, 2005-2008," *JAMA*, vol. 304, no. 6, pp. 649–656, 2010.

[6] A. Das, P. G. McGuire, and S. Rangasamy, "Diabetic macular edema: pathophysiology and novel therapeutic targets," *Ophthalmology*, vol. 122, no. 7, pp. 1375–1394, 2015.

[7] P. Romero-Aroca, M. Baget-Bernaldiz, A. Pareja-Rios, M. Lopez-Galvez, R. Navarro-Gil, and R. Verges, "Diabetic macular edema pathophysiology: vasogenic versus inflammatory," *Journal Diabetes Research*, vol. 2016, article 2156273, pp. 1–17, 2016.

[8] N. Dong, B. Xu, L. Chu, and X. Tang, "Study of 27 aqueous humor cytokines in type 2 diabetic patients with or without macular edema," *PLoS One*, vol. 10, no. 4, article e0125329, 2015.

[9] M. C. Sabaner, M. Akdogan, M. Doğan et al., "Inflammatory cytokines, oxidative and antioxidative stress levels in patients with diabetic macular edema and hyperreflective spots," *European Journal of Ophthalmology*, p. 112067212096205, 2020.

[10] R. Crosby-Nwaobi, I. Chatziralli, T. Sergentanis, T. Dew, A. Forbes, and S. Sivaprasad, "Cross talk between lipid metabolism and inflammatory markers in patients with diabetic retinopathy," *Journal Diabetes Research*, vol. 2015, article 191382, pp. 1–9, 2015.

[11] M. Sasaki, R. Kawasaki, J. E. Noonan, T. Y. Wong, E. Lamoureux, and J. J. Wang, "Quantitative measurement of hard exudates in patients with diabetes and their associations with serum lipid levels," *Investigative Ophthalmology & Visual Science*, vol. 54, no. 8, pp. 5544–5550, 2013.

[12] R. Benarous, M. B. Sasongko, S. Qureshi et al., "Differential association of serum lipids with diabetic retinopathy and diabetic macular edema," *Investigative Ophthalmology & Visual Science*, vol. 52, no. 10, pp. 7464–7469, 2011.

[13] M. Figueras-Roca, B. Molins, A. Sala-Puigdollers et al., "Peripheral blood metabolic and inflammatory factors as

biomarkers to ocular findings in diabetic macular edema," *PLoS One*, vol. 12, no. 3, article e0173865, 2017.

[14] M. Figueras-Roca, J. Matas, V. Llorens et al., "Systemic contribution of inflammatory mediators to the severity of diabetic and uveitic macular edema," *Graefe's Archive for Clinical and Experimental Ophthalmology*, 2021.

[15] P. Phadikar, S. Saxena, S. Ruia, T. Y. Lai, C. H. Meyer, and D. Eliott, "The potential of spectral domain optical coherence tomography imaging based retinal biomarkers," *International Journal of Retina and Vitreous*, vol. 3, no. 1, 2017.

[16] J. Vira, A. Marchese, R. B. Singh, and A. Agarwal, "Swept-source optical coherence tomography imaging of the retinochoroid and beyond," *Expert Review of Medical Devices*, vol. 17, no. 5, pp. 413–426, 2020.

[17] M. V. Cicinelli, M. Cavalleri, M. Brambati, R. Lattanzio, and F. Bandello, "New imaging systems in diabetic retinopathy," *Acta Diabetologica*, vol. 56, no. 9, pp. 981–994, 2019.

[18] K. Y. Tey, K. Teo, A. C. S. Tan et al., "Optical coherence tomography angiography in diabetic retinopathy: a review of current applications," *Eye and Vision*, vol. 6, no. 1, 2019.

[19] S. Ghosh, P. Bansal, H. Shejao, R. Hegde, D. Roy, and S. Biswas, "Correlation of morphological pattern of optical coherence tomography in diabetic macular edema with systemic risk factors in middle aged males," *International Ophthalmology*, vol. 35, no. 1, pp. 3–10, 2015.

[20] C. P. Wilkinson, Ferris FL 3rd, R. E. Klein et al., "Proposed international clinical diabetic retinopathy and diabetic macular edema disease severity scales," *Ophthalmology*, vol. 110, no. 9, pp. 1677–1682, 2003.

[21] Y. J. S. Chopra, T. S. Lim, S. A. Cha et al., "Lipoprotein(a) predicts the development of diabetic retinopathy in people with type 2 diabetes mellitus," *Journal of Clinical Lipidology*, vol. 10, pp. 426–433, 2016.

[22] H. Funatsu, E. Shimizu, H. Noma, T. Mimura, and S. Hori, "Association between serum lipoprotein (a) level and progression of non-proliferative diabetic retinopathy in type 2 diabetes," *Acta Ophthalmologica*, vol. 87, no. 5, pp. 501–505, 2009.

[23] R. Chopra, J. G. Saramma, J. Mary, and A. Rebecca, "Lipoprotein(a) as a risk factor for diabetic retinopathy in patients with type 2 diabetes mellitus," *Indian Journal of Ophthalmology*, vol. 55, no. 3, pp. 195–198, 2007.

[24] B. Guerci, L. Meyer, S. Sommer et al., "Severity of diabetic retinopathy is linked to lipoprotein (a) in type 1 diabetic patients," *Diabetes & Metabolism*, vol. 25, no. 5, pp. 412–418, 1999.

[25] W. J. Tu, H. Liu, Q. Liu, J. L. Cao, and M. Guo, "Association between serum lipoprotein(a) and diabetic retinopathy in Han Chinese patients with type 2 diabetes," *The Journal of Clinical Endocrinology and Metabolism*, vol. 102, no. 7, pp. 2525–2532, 2017.

[26] S. N. Sotiriou, V. V. Orlova, N. Al-Fakhri et al., "Lipoprotein(a) in atherosclerotic plaques recruits inflammatory cells through interaction with Mac-1 integrin," *The FASEB Journal*, vol. 20, no. 3, pp. 559–561, 2006.

[27] S. Tsimikas and J. L. Hall, "Lipoprotein(a) as a potential causal genetic risk factor of cardiovascular disease: a rationale for increased efforts to understand its pathophysiology and develop targeted therapies," *Journal of the American College of Cardiology*, vol. 60, no. 8, pp. 716–721, 2012.

[28] H. D. Wu, L. Berglund, C. Dimayuga et al., "High lipoprotein(a) levels and small apolipoprotein(a) sizes are associated with endothelial dysfunction in a multiethnic cohort," *Journal of the American College of Cardiology*, vol. 43, no. 10, pp. 1828–1833, 2004.

[29] A. J. Jenkins, T. J. Lyons, D. Zheng et al., "Lipoproteins in the DCCT/EDIC cohort: associations with diabetic nephropathy," *Kidney International*, vol. 64, no. 3, pp. 817–828, 2003.

[30] R. J. Woodman, G. F. Watts, D. A. Playford, J. D. Best, and D. C. Chan, "Oxidized LDL and small LDL particle size are independently predictive of a selective defect in microcirculatory endothelial function in type 2 diabetes," *Diabetes, Obesity & Metabolism*, vol. 7, no. 5, pp. 612–617, 2005.

[31] R. H. Muni, R. P. Kohly, E. Q. Lee, J. E. Manson, R. D. Semba, and D. A. Schaumberg, "Prospective study of inflammatory biomarkers and risk of diabetic retinopathy in the diabetes control and complications trial," *JAMA Ophthalmology*, vol. 131, no. 4, pp. 514–521, 2013.

[32] B. N. Alamri, A. Bahabri, A. A. Aldereihim et al., "Hyperglycemia effect on red blood cells indices," *European Review for Medical and Pharmacological Sciences*, vol. 23, no. 5, pp. 2139–2150, 2019.

[33] Y. Wang, P. Yang, Z. Yan et al., "The relationship between erythrocytes and diabetes mellitus," *Journal Diabetes Research*, vol. 2021, article 6656062, pp. 1–9, 2021.

[34] A. V. Buys, M. J. Van Rooy, P. Soma, D. Van Papendorp, B. Lipinski, and E. Pretorius, "Changes in red blood cell membrane structure in type 2 diabetes: a scanning electron and atomic force microscopy study," *Cardiovascular Diabetology*, vol. 12, no. 1, p. 25, 2013.

[35] C. Framme, S. Wolf, and U. Wolf-Schnurrbusch, "Small dense particles in the retina observable by spectral-domain optical coherence tomography in age-related macular degeneration," *Investigative Ophthalmology & Visual Science*, vol. 51, no. 11, pp. 5965–5969, 2010.

[36] G. Coscas, F. Coscas, S. Vismara, E. Souied, and G. Soubrane, "Tomographie par coherence optique de type Spectral Domain dans la degenerescence maculaire liee a l'age:," *Journal Français d'Ophtalmologie*, vol. 31, no. 4, pp. 353–361, 2008.

[37] J. Fest, R. Ruiter, M. A. Ikram, T. Voortman, C. H. J. van Eijck, and B. H. Stricker, "Reference values for white blood-cell-based inflammatory markers in the Rotterdam Study: a population-based prospective cohort study," *Scientific Reports*, vol. 8, no. 1, p. 10566, 2018.

[38] S. Rangasamy, P. G. McGuire, C. Franco Nitta, F. Monickaraj, S. R. Oruganti, and A. Das, "Chemokine mediated monocyte trafficking into the retina: role of inflammation in alteration of the blood-retinal barrier in diabetic retinopathy," *PLoS One*, vol. 9, no. 10, article e108508, 2014.

[39] S. Vujosevic and E. Midena, "Retinal layers changes in human preclinical and early clinical diabetic retinopathy support early retinal neuronal and Müller cells alterations," *Journal Diabetes Research*, vol. 2013, article 905058, pp. 1–8, 2013.

[40] S. Omri, F. Behar-Cohen, Y. de Kozak et al., "Microglia/macrophages migrate through retinal epithelium barrier by a transcellular route in diabetic retinopathy: role of PKCζ in the Goto Kakizaki rat model," *The American Journal of Pathology*, vol. 179, no. 2, pp. 942–953, 2011.

[41] I. P. Chatziralli, T. N. Sergentanis, and S. Sivaprasad, "Hyper-reflective foci as an independent visual outcome predictor in macular edema due to retinal vascular diseases treated with intravitreal dexamethasone or ranibizumab," *Retina*, vol. 36, no. 12, pp. 2319–2328, 2016.

[42] K. Turkmen, F. Ozcicek, A. Ozcicek, E. M. Akbas, F. M. Erdur, and H. Z. Tonbul, "The relationship between neutrophil-to-lymphocyte ratio and vascular calcification in end-stage renal disease patients," *Hemodialysis International*, vol. 18, no. 1, pp. 47–53, 2014.

[43] A. Ahsen, M. S. Ulu, S. Yuksel et al., "As a new inflammatory marker for familial Mediterranean fever: neutrophil-to-lymphocyte ratio," *Inflammation*, vol. 36, no. 6, pp. 1357–1362, 2013.

[44] A. Dursun, S. Ozturk, H. Yucel et al., "Association of neutrophil/lymphocyte ratio and retinal vein occlusion," *European Journal of Ophthalmology*, vol. 25, no. 4, pp. 343–346, 2015.

[45] N. Ilhan, M. C. Daglioglu, O. Ilhan et al., "Assessment of neutrophil/lymphocyte ratio in patients with age-related macular degeneration," *Ocular Immunology and Inflammation*, vol. 23, no. 4, pp. 287–290, 2015.

[46] B. E. Kurtul and P. A. Ozer, "The relationship between neutrophil-to-lymphocyte ratio and age-related macular degeneration," *Korean Journal of Ophthalmology*, vol. 30, no. 5, pp. 377–381, 2016.

[47] S. M. Ulu, M. Dogan, A. Ahsen et al., "Neutrophil-to-lymphocyte ratio as a quick and reliable predictive marker to diagnose the severity of diabetic retinopathy," *Diabetes Technology & Therapeutics*, vol. 15, no. 11, pp. 942–947, 2013.

[48] A. Bolayir, S. F. Gokce, B. Cigdem et al., "Monocyte/high-density lipoprotein ratio predicts the mortality in ischemic stroke patients," *Neurologia i Neurochirurgia Polska*, vol. 52, no. 2, pp. 150–155, 2018.

[49] E. Aydin, I. Ates, M. Fettah Arikan, N. Yilmaz, and F. Dede, "The ratio of monocyte frequency to HDL cholesterol level as a predictor of asymptomatic organ damage in patients with primary hypertension," *Hypertension Research*, vol. 40, no. 8, pp. 758–764, 2017.

[50] P. Ancuta, J. Wang, and D. Gabuzda, "CD16+monocytes produce IL-6, CCL2, and matrix metalloproteinase-9 upon interaction with CX3CL1-expressing endothelial cells," *Journal of Leukocyte Biology*, vol. 80, no. 5, pp. 1156–1164, 2006.

[51] A. J. Murphy and K. J. Woollard, "High-density lipoprotein: a potent inhibitor of inflammation," *Clinical and Experimental Pharmacology & Physiology*, vol. 37, no. 7, pp. 710–718, 2010.

[52] G. Şatırtav, E. Mirza, R. Oltulu, G. D. Mirza, and H. Kerimoğlu, "Assessment of monocyte/HDL ratio in branch retinal vein occlusion," *Ocular Immunology and Inflammation*, vol. 28, no. 3, pp. 463–467, 2020.

[53] D. L. E. Villanueva, M. D. Tiongson, J. D. Ramos, and E. J. Llanes, "Monocyte to high-density lipoprotein ratio (MHR) as a predictor of mortality and major adverse cardiovascular events (MACE) among ST elevation myocardial infarction (STEMI) patients undergoing primary percutaneous coronary intervention: a meta-analysis," *Lipids in Health and Disease*, vol. 19, no. 1, p. 55, 2020.

[54] G. Ceyhun and M. Ç. Engin, "The monocyte/high density lipoprotein cholesterol ratio (MHR) as an indicator of the need for amputation in patients with peripheral artery disease developing critical limb ischemia," *Angiology*, vol. 72, no. 3, pp. 268–273, 2021.